

**Bounds on Flexural Properties and Buckling Response for Symmetrically  
Laminated Plates**

*Paul M. Weaver\**

*Queen's Building*

*Dept. of Aerospace Engineering*

*University of Bristol, BS8 1TR, UK*

*Fax: 44-117-928-2771*

*e-mail: paul.weaver@bristol.ac.uk*

*and*

*Michael P. Nemeth*

*Mechanics of Structures and Materials Branch*

*NASA Langley Research Center, Hampton, Virginia USA*

**Abstract**

Nondimensional parameters and equations governing the buckling behavior of rectangular symmetrically laminated plates are presented that can be used to represent the buckling resistance, for plates made of all known structural materials, in a very general, insightful, and encompassing manner. In addition, these parameters can be used to assess the degree of plate orthotropy, to assess the importance of anisotropy that couples bending and twisting deformations, and to characterize quasi-isotropic laminates

---

\* Corresponding author

quantitatively. Bounds for these nondimensional parameters are also presented that are based on thermodynamics and practical laminate construction considerations. These bounds provides insight into potential gains in buckling resistance through laminate tailoring and composite-material development. As an illustration of this point, upper bounds on the buckling resistance of long rectangular orthotropic plates with simply supported or clamped edges and subjected to uniform axial compression, uniform shear, or pure inplane bending loads are presented. The results indicate that the maximum gain in buckling resistance for tailored orthotropic laminates, with respect to the corresponding isotropic plate, is in the range of 26-36% for plates with simply supported edges, irrespective of the loading conditions. For the plates with clamped edges, the corresponding gains in buckling resistance are in the range of 9-12% for plates subjected to compression or pure inplane bending loads and potentially up to 30% for plates subjected to shear loads.

## **Introduction**

Laminated composite materials lend themselves to elastic tailoring of anisotropic structural components - a feature that allows structural designers to customize the stiffness-critical response of structural elements such as flat plates and curved panels. The benefits of elastic tailoring are usually manifested as a reduction in structural weight or improved performance, which are very important to many widespread applications such as aircraft, spacecraft, and sporting goods. Typically, these benefits are obtained by simply ensuring that the laminate stiffnesses are different in the principal directions (an

example of orthotropy), or by building in elements of anisotropy that couple response modes to obtain a desired effect (e.g., coupling of extension, contraction and inplane shear deformations). The type of anisotropy that is considered in the present study is the anisotropy associated with the coupling of pure-bending and twisting deformations of symmetrically laminated flat plates. For convenience, this type of anisotropy is referred to herein as flexural anisotropy.

Most aerospace design practices limit the use of polymeric, laminated composites to those that are balanced and symmetrically laminated. The balanced-laminate requirement eliminates anisotropy associated with coupling between inplane extension or contraction and inplane shearing deformations. In contrast, the symmetric-laminate requirement eliminates anisotropy associated with coupling between inplane extension, contraction, or shear with bending or twisting deformations. These laminate-construction design requirements are mostly done to simplify the structural response or to prevent residual stresses from altering the structural shape during curing. However, these limitations on laminate construction generally do not eliminate flexural anisotropy. This point is important because it has been shown that in some cases flexural anisotropy may significantly influence the buckling resistance of laminated-composite plates (Chamis, 1969; Nemeth, 1986, Grenestedt, 1991). As such, it is useful to characterize the effects of flexural anisotropy on buckling behavior. The nondimensional stiffness parameters popularized by Nemeth, and used to conduct extensive parametric studies of the buckling behavior of simply supported and clamped laminated-composite plates, serve this purpose (Nemeth, 1992a, 1995, and 1997). It has been shown by Nemeth that

the buckling behavior of simply supported and clamped rectangular plates that are symmetrically laminated can be completely characterized by these nondimensional parameters, in a general manner amenable to the development of concise design data. Unfortunately, these nondimensional parameters generally vary in a coupled manner with changes in laminate construction and their bounding values are only partially known (Weaver, 2003 and 2004). Knowing the bounds on these nondimensional parameters is important because it limits the size of the design space, which has practical implications to designers and design-data developers.

The objective of the present study is to determine the practical upper and lower bounds of basically the nondimensional parameters, presented by Nemeth, in order to gain insight into bounds on the buckling resistance of rectangular plates made of existing materials and, possibly, to gain insight into the potential benefits of new material development. To accomplish this objective, background information on the nondimensional parameters and equations governing buckling is presented first. Then, lower bounds to the values of the nondimensional parameters are determined from thermodynamic considerations and upper bounds are derived from practical laminate construction considerations. Finally, upper bounds to the buckling resistance of infinitely long, orthotropic flat plates are presented. In particular, rectangular plates that are subjected to either uniform axial compression, shear, or pure inplane bending loads and with either simply supported or clamped unloaded edges are considered.

## **Background**

It is well known that useful nondimensional parameters can be obtained by normalising the equations that govern the response in a manner that renders the fewest number of parameters needed to completely characterize the response. For example, studies that have adopted this approach to better understand buckling, vibration, and flutter of plates are Huber (1929); Wittrick (1952), Shulesko (1957), Stein (1983); Brunelle (1983, 1985 and 1986); Oyibo and Berman (1985); Yang and Kuo (1986); Nemeth (1986, 1992b, and 1994); and Geier and Singh (1997). For a rectangular plate of width  $b$ , defined by an  $x$ - $y$  coordinate system (see Fig. 1), the plate buckling behavior is governed by

$$\begin{aligned} D_{11} \frac{\partial^4 w}{\partial x^4} + 2(D_{12} + 2D_{66}) \frac{\partial^4 w}{\partial^2 x \partial y^2} + D_{22} \frac{\partial^4 w}{\partial y^4} + 4D_{16} \frac{\partial^4 w}{\partial^3 x \partial y} + 4D_{26} \frac{\partial^4 w}{\partial x \partial y^3} \\ + N_x \frac{\partial^2 w}{\partial x^2} + N_y \frac{\partial^2 w}{\partial y^2} + 2N_{xy} \frac{\partial^2 w}{\partial x \partial y} = 0 \end{aligned} \quad (1)$$

where the subscripted  $D$ -terms are the flexural stiffnesses of classical laminated-plate theory,  $w$  is the transverse displacement and the functions  $N_x$ ,  $N_y$  and  $N_{xy}$  are internal in-plane stress resultants where compression is positive and positive shear corresponds to the boundary tractions shown in Fig. 1. Following Nemeth (1986 and 1994), it is convenient to nondimensionalize the form of Eq. (1) by redefining the co-ordinates as

$\xi = \frac{x}{\lambda}$  and  $\eta = \frac{y}{b}$  and multiplying throughout by  $b^2 \lambda^2 / \sqrt{D_{11} D_{22}}$  to obtain

$$\begin{aligned} & \frac{1}{\alpha^{*2}} \frac{\partial^4 w}{\partial \xi^4} + 2\beta \frac{\partial^4 w}{\partial \xi^2 \partial \eta^2} + \alpha^{*2} \frac{\partial^4 w}{\partial \eta^4} \\ & + 4 \frac{\gamma}{\alpha^*} \frac{\partial^4 w}{\partial \xi^3 \partial \eta} + 4\delta \alpha^* \frac{\partial^4 w}{\partial \xi \partial \eta^3} + \pi^2 \left\{ n_x \frac{\partial^2 w}{\partial \xi^2} + \alpha^{*2} n_y \frac{\partial^2 w}{\partial \eta^2} - 2\alpha^* n_{xy} \frac{\partial^2 w}{\partial \xi \partial \eta} \right\} = 0 \end{aligned} \quad (2)$$

where  $\lambda$  is a characteristic length and is usually chosen as the buckling half-wavelength.

The nondimensionalized parameters in Eq. (2) are given by

$$\alpha^* = \frac{\lambda}{b} \sqrt[4]{\frac{D_{22}}{D_{11}}}; \quad \beta = \frac{(D_{12} + 2D_{66})}{(D_{11}D_{22})^{1/2}}; \quad \gamma = \frac{D_{16}}{(D_{11}^3 D_{22})^{1/4}}; \quad \delta = \frac{D_{26}}{(D_{22}^3 D_{11})^{1/4}} \quad (3a)$$

$$n_x = \frac{N_x b^2}{\pi^2 \sqrt{D_{11}D_{22}}}; \quad n_y = \frac{N_y b^2}{\pi^2 D_{22}}; \quad n_{xy} = \frac{N_{xy} b^2}{\pi^2 (D_{11}D_{22}^3)^{1/4}} \quad (3b)$$

where  $\alpha^*$  and  $\beta$  are flexural-orthotropy parameters,  $\delta$  and  $\gamma$  are flexural-anisotropy parameters, and  $n_x$ ,  $n_y$ , and  $n_{xy}$  are nondimensional stress resultants whose critical values are well-known as buckling coefficients. It is worth noting that  $\alpha^*$  is the reciprocal of the corresponding parameter originally defined by Nemeth (1986) and has a physical interpretation as a stiffness-weighted buckle aspect ratio for infinitely long plates or a stiffness-weighted plate aspect ratio for finite-length plates. Likewise, the ratio of the principal bending stiffnesses is defined herein as  $\alpha = \sqrt[4]{D_{22}/D_{11}}$  for convenience in the discussion that follows. The term  $\beta$  was originally introduced by Seydel (1933) (as the reciprocal of  $\beta$ ) and was also used by Brunelle and Oyibo (1983).

As one might expect, there are many ways of nondimensionalizing the plate bending stiffness parameters, but done in this way is particularly useful. For example, for isotropic materials the flexural-orthotropy parameters  $\alpha$  and  $\beta$  take on values of unity and the flexural-anisotropy parameters  $\delta$  and  $\gamma$  are zero valued. Furthermore, for simply supported and clamped plates the number of flexural-orthotropy parameters has been reduced from four dimensional stiffnesses to two nondimensional stiffness measures - a feature that greatly simplifies laminate design.

The nondimensional parameters presented in Eq. (3a) and the stiffness ratio  $\alpha = \sqrt[4]{D_{22}/D_{11}}$  are also useful in the design of special-purpose laminates when used in conjunction with the concept of a quasi-isotropic laminate (Tsai and Pagano, 1968) as a baseline or starting configuration that behaves similar to a corresponding homogeneous isotropic plate. For this class of laminate constructions, the inplane stiffness and response characteristics are identical to those for the corresponding isotropic materials. In slight contrast, the bending and twisting stiffness and response characteristics are somewhat different than those for the corresponding isotropic materials. These differences are conveniently represented with the nondimensional parameters given by Eq. (3a). For example, Nemeth (1992a) showed that values for  $\alpha$  and  $\beta$  approach a value of unity, and the values for  $\delta$  and  $\gamma$  approach zero, in a monotonic manner as the number of plies in a quasi-isotropic laminate increases. Thus, the nondimensional parameters provide a means for quantitatively assessing how different a given quasi-isotropic laminate is from a homogeneous isotropic material. In the context of design, stiffness tailoring may be viewed as perturbing the values of these nondimensional parameters from the values for

an isotropic material to obtain a desired response. It is important to note that different laminate constructions that possess identical values for  $\alpha$ ,  $\beta$ ,  $\delta$ , and  $\gamma$  will exhibit identical response characteristics when these parameters govern the structural behavior. Thus, it is important to know the practical bounds on  $\alpha$ ,  $\beta$ ,  $\delta$ , and  $\gamma$  for a wide range of lamina material systems in order to determine the potential for performance enhancements that are possible by using elastic tailoring.

### **Thermodynamic Considerations**

Positiveness of the strain energy density is a fundamental consideration in structural mechanics. In particular, the energy stored by an elastic body during deformation is a positive-valued quantity that can be converted into work. It is physically impossible for an elastic body to either not store or to dissipate strain energy during deformation. This physical consideration places constraints on the values of  $\alpha$ ,  $\beta$ ,  $\delta$ , and  $\gamma$ . These constraints are derived subsequently.

Mansfield (1989) gives the expression for the total strain energy,  $U_b$ , of a flat flexurally anisotropic plate undergoing bending and twisting deformations as

$$U_b = \frac{1}{2} \iint_A \{\kappa\}^T [D] \{\kappa\} dx dy \quad (4a)$$

or in expanded form, as



$$U_b = \frac{1}{2} \iint_A \left\{ \begin{aligned} &D_{11} \frac{\partial^2 w}{\partial x^2} \frac{\partial^2 w}{\partial x^2} + 2D_{12} \frac{\partial^2 w}{\partial x^2} \frac{\partial^2 w}{\partial y^2} + D_{22} \frac{\partial^2 w}{\partial y^2} \frac{\partial^2 w}{\partial y^2} \\ &+ 4 \frac{\partial^2 w}{\partial x \partial y} \left( D_{16} \frac{\partial^2 w}{\partial y^2} + D_{26} \frac{\partial^2 w}{\partial x^2} + D_{66} \frac{\partial^2 w}{\partial x \partial y} \right) \end{aligned} \right\} dx dy \quad (4b)$$

with

$$\{\kappa\}^T = \left\{ -\frac{\partial^2 w}{\partial x^2}, -\frac{\partial^2 w}{\partial y^2}, -2 \frac{\partial^2 w}{\partial x \partial y} \right\} \quad (5)$$

and

$$[D] = \begin{bmatrix} D_{11} & D_{12} & D_{16} \\ D_{12} & D_{22} & D_{26} \\ D_{16} & D_{26} & D_{66} \end{bmatrix} \quad (6)$$

where  $\{\kappa\}$  is the vector of curvatures and twist, given in terms of transverse displacements  $w$  and the independent plate variables  $(x, y)$ . To obtain a convenient nondimensional form of the total strain energy, the stiffness matrix  $[D]$  is nondimensionalized following the procedure outlined previously and yields

$$\begin{bmatrix} D_{11} & D_{12} & D_{16} \\ D_{12} & D_{22} & D_{26} \\ D_{16} & D_{26} & D_{66} \end{bmatrix} = \sqrt{D_{11} D_{22}} \begin{bmatrix} \alpha^2 & \nu_f & \alpha \gamma \\ \nu_f & \frac{1}{\alpha^2} & \frac{\delta}{\alpha} \\ \alpha \gamma & \frac{\delta}{\alpha} & \frac{\beta - \nu_f}{2} \end{bmatrix} \quad (7)$$

where the additional nondimensional parameter  $\nu_f$  is

$$\nu_f = \frac{D_{12}}{\sqrt{D_{11}D_{22}}} \quad (8)$$

The parameter  $\nu_f$ , introduced by Brunelle and Oyibo (1983), represents the geometric mean of the two principal Poisson's ratio effects, associated with pure bending, that is, a mean anticlastic bending effect.

Typically, in defining the conditions on the elastic material parameters, positive definiteness of the strain energy density is enforced, which is valid at every material point of a structure. Enforcing this condition on the integrand of Eq. (4) results in the requirement that the matrix defined by Eq. (7) be a positive-definite matrix, which yields relationships that  $\alpha$ ,  $\beta$ ,  $\delta$ ,  $\gamma$  and  $\nu_f$  must obey. Applying Sylvester's criteria for positive definiteness of a matrix yields the following requirements (Zwillinger, 1996):

$$\begin{aligned} \alpha &> 0 \\ (1 - \nu_f^2) &> 0 \\ \beta - \nu_f &> 0 \\ \beta - \nu_f - 2\gamma^2 &> 0 \\ \beta - \nu_f - 2\delta^2 &> 0 \\ \left( \frac{\beta - \nu_f}{2} - \delta^2 \right) - \nu_f \left( \nu_f \left( \frac{\beta - \nu_f}{2} \right) - \delta\gamma \right) + \alpha\gamma^2(\nu_f\delta - \gamma) &> 0 \end{aligned} \quad (9)$$

The second and third of these conditions give the following bounds on  $\nu_f$  and  $\beta$ , that is,

$$-1 < \nu_f < 1 \text{ and } \beta > -1 \quad (10)$$

Because no apparent upper bound on  $\beta$  is given by Eqs. (9), bounds for  $\gamma$  and  $\delta$  are also not apparent. As a result, in the present study, bounds on the nondimensional parameters are sought with respect to the buckling response of simply supported and clamped plates, not the material behavior. For this class of problems, the buckling response is completely independent of  $\nu_f$  and positiveness of the total strain energy is used, instead of positive definiteness of the strain energy density, to eliminate  $\nu_f$  from consideration. Specifically, a modified form of the total strain energy is sought that is independent of  $\nu_f$  and whose positiveness can be guaranteed by enforcing positive definiteness of the corresponding integrand. Thus, an alternate form of Eq. (4), the total strain energy of a plate, is used that produces structural-response bounds on the minimum number of nondimensional parameters required to characterize the buckling behavior of simply supported and clamped plates as follows.

The desired form of Eq. (4b) is obtained by noting that it is possible to eliminate  $\nu_f$  as a variable governing the structural response for several cases of practical interest in design; that is, plates for which the transverse buckling displacement  $w = 0$  on the boundary (e.g., see the results presented in Nemeth (1992a)). This simplification is done by integrating Eq. (4b) by parts using Green's Theorem and enforcing  $w = 0$  on the boundary of a finite-length plate or the periodic unit of an infinitely long plate to obtain

$$\iint \frac{\partial^2 w}{\partial x^2} \frac{\partial^2 w}{\partial y^2} dx dy = \iint \left( \frac{\partial^2 w}{\partial x \partial y} \right)^2 dx dy \quad (11)$$

Using this expression, the strain energy components containing  $\beta$  and  $\nu_f$  may be reduced to a single term in  $\beta$ ; that is,

$$\iint \left[ 2\nu_f \frac{\partial^2 w}{\partial x^2} \frac{\partial^2 w}{\partial y^2} + 2(\beta - \nu_f) \left( \frac{\partial^2 w}{\partial x \partial y} \right)^2 \right] dx dy = \iint \left[ 2\beta \frac{\partial^2 w}{\partial x^2} \frac{\partial^2 w}{\partial y^2} \right] dx dy \quad (12a)$$

or

$$\iint \left[ 2\nu_f \frac{\partial^2 w}{\partial x^2} \frac{\partial^2 w}{\partial y^2} + 2(\beta - \nu_f) \left( \frac{\partial^2 w}{\partial x \partial y} \right)^2 \right] dx dy = \iint \left[ 2\beta \left( \frac{\partial^2 w}{\partial x \partial y} \right)^2 \right] dx dy \quad (12b)$$

which allows the total strain energy to be written as

$$\frac{U_b}{\sqrt{D_{11}D_{22}}} = \frac{1}{2} \iint_A \{\kappa\}^T [D_{\text{mod}}] \{\kappa\} dx dy \quad (13)$$

where  $[D_{\text{mod}}]$  is a modified nondimensional stiffness matrix that is given by

$$[D_{\text{mod}}] = \begin{bmatrix} \alpha^2 & \beta & \alpha\gamma \\ \beta & \frac{1}{\alpha^2} & \frac{\delta}{\alpha} \\ \alpha\gamma & \frac{\delta}{\alpha} & 0 \end{bmatrix} \quad (14a)$$

or by

$$[D_{\text{mod}}] = \begin{bmatrix} \alpha^2 & 0 & \alpha\gamma \\ 0 & \frac{1}{\alpha^2} & \frac{\delta}{\alpha} \\ \alpha\gamma & \frac{\delta}{\alpha} & \frac{\beta}{2} \end{bmatrix} \quad (14b)$$

depending on whether coefficients of  $\frac{\partial^2 w}{\partial x^2} \frac{\partial^2 w}{\partial y^2}$  or  $\left(\frac{\partial^2 w}{\partial x \partial y}\right)^2$  are retained in the strain energy, respectively. Neither representation of  $[D_{\text{mod}}]$  is satisfactory for the purpose of finding bounds by enforcing positive definiteness of the integrand, however, as the former has a value of zero for a leading diagonal term, which is impossible for the requirement of positive strain energy, whilst the latter does provide for the contribution of  $\frac{\partial^2 w}{\partial x^2} \frac{\partial^2 w}{\partial y^2}$  in its representation of strain energy. It is more useful to represent the strain energy associated with  $\beta$  as a linear combination of the terms given by Eqs. (12); that is,

$$\left\{ \iint \left[ 2\beta \frac{\partial^2 w}{\partial x^2} \frac{\partial^2 w}{\partial y^2} \right] dx dy = \iint \left[ 2\beta \left( \frac{\partial^2 w}{\partial x \partial y} \right)^2 \right] dx dy \right\} = \iint 2\beta \left[ 2m \left( \frac{\partial^2 w}{\partial x \partial y} \right)^2 + n \frac{\partial^2 w}{\partial x^2} \frac{\partial^2 w}{\partial y^2} \right] dx dy \quad (15a)$$

which allows the strain energy to be represented as

$$\frac{U_b}{\sqrt{D_{11}D_{22}}} = \frac{1}{2} \iint_A \{\kappa\}^T [D^*_{\text{mod}}] \{\kappa\} dx dy \quad (15b)$$

where  $[D^*_{\text{mod}}]$  is another modified nondimensional stiffness matrix that is given by

$$[D^*_{\text{mod}}] = \begin{bmatrix} \alpha^2 & n\beta & \alpha\gamma \\ n\beta & \frac{1}{\alpha^2} & \frac{\delta}{\alpha} \\ \alpha\gamma & \frac{\delta}{\alpha} & m\beta \end{bmatrix} \quad (16)$$

for which  $2m + n = 1$  must be satisfied in order for Eqs. (13) and (15b) to remain equivalent, where  $m$  and  $n$  are real-valued numbers. The modified stiffness matrix

$[D^*_{\text{mod}}]$  is more general than  $[D_{\text{mod}}]$  because assumptions have not been made

concerning the relative contribution of  $\beta$  to  $\frac{\partial^2 w}{\partial x^2} \frac{\partial^2 w}{\partial y^2}$  or  $\left(\frac{\partial^2 w}{\partial x \partial y}\right)^2$ .

A sufficient condition for positive-valued total strain energy of deformation is that the modified stiffness matrix  $[D^*_{\text{mod}}]$  be positive definite. Applying Sylvester's criteria, once again, for positive definiteness of a matrix yields the following requirements:

$$\begin{aligned}
 \alpha &> 0 \\
 m\beta &> 0 \\
 (n\beta)^2 &< 1 \\
 m\beta &> \delta^2 \\
 m\beta &> \gamma^2 \\
 -mn^2\beta^3 + (2n\delta\gamma + m)\beta - (\gamma^2 + \delta^2) &> 0
 \end{aligned} \tag{17}$$

Combining the latter of these relationships with  $2m + n = 1$  results in the following cubic polynomial in  $n\beta$

$$\frac{(n\beta)^3}{2} - \frac{\beta(n\beta)^2}{2} + \left(2\gamma\delta - \frac{1}{2}\right)(n\beta) + \left(\frac{\beta}{2} - \delta^2 - \gamma^2\right) > 0 \tag{18}$$

For any given values of  $\delta$  and  $\gamma$ , Eq. (18) gives the minimum, value of  $\beta$  that corresponds to positive strain energy. Its dependency on  $n$  is of little consequence because the minimum value of  $\beta$  is determined directly by ensuring that the solution to Eq. (18) has three real-valued roots, which, in turn, is satisfied by ensuring that the discriminant of the third-order polynomial in Eq. (18) is zero; that is,

$$\frac{1}{27}\left(4\gamma\delta - \frac{\beta^2}{3} - 1\right)^3 + \frac{1}{4}\left(2\gamma^2 + 2\delta^2 - \frac{2}{3}\beta - \frac{4}{3}\gamma\delta\beta + \frac{2}{27}\beta^3\right)^2 = 0 \quad (19)$$

which is independent of the parameters  $m$  and  $n$ . Simplification of Eq. (19) yields a fourth-order expression in  $\beta$  given by

$$\begin{aligned} & \frac{\beta^4}{27} - \frac{2}{27}(\gamma^2 + \delta^2)\beta^3 - \frac{1}{27}(2 + 20\gamma\delta - 4\gamma^2\delta^2)\beta^2 + \frac{1}{3}(4\gamma^3\delta + 2\gamma^2 + 2\delta^2 + 4\delta^3\gamma)\beta \\ & + \left(\frac{1}{27} - \gamma^4 - \delta^4 - \frac{2}{9}\gamma^2\delta^2 - \frac{4}{9}\gamma\delta - \frac{64}{27}\gamma^3\delta^3\right) = 0 \end{aligned} \quad (20)$$

Equation (20) is used herein to obtain the minimum value of  $\beta$  for given values of  $\delta$  and  $\gamma$ . It is noted that for some values of  $\delta$  and  $\gamma$  there are multiple solutions for  $\beta$  that satisfy Eq. (20). For these circumstances, the appropriate choice of the minimal  $\beta$  value is the one that also satisfies the thermodynamic conditions given in Eq.(17), and by so doing, provides a unique solution for  $\beta$ . Upon finding the minimal value for  $\beta$ , Eq. (18) is used to determine the value of the parameter  $n$ . It is useful to observe that Eq. (20) exhibits identical dependence on  $\delta$  and  $\gamma$ , meaning that  $\delta$  and  $\gamma$  have identical effects on the minimal value of  $\beta$  because they are interchangeable. The contours of minimal  $\beta$ , as given by Eq. (20), are depicted as a function of  $\delta$  and  $\gamma$  in Fig. 2. Minimal  $\beta$  values are also listed in Tables 1a and 1b, and may prove to be useful in formulating parametric studies.

**Table 1a.** Minimum values of  $\beta$  for given values of  $\delta$  and  $\gamma$ . a)  $-0.99 < \gamma < 0$  and  $-0.99$

$< \delta < 0.99$

$\gamma$	<b>-0.99</b>	<b>-0.9</b>	<b>-0.8</b>	<b>-0.7</b>	<b>-0.6</b>	<b>-0.5</b>	<b>-0.4</b>	<b>-0.3</b>	<b>-0.2</b>	<b>-0.1</b>	<b>0</b>
$\delta$											
<b>-0.99</b>	<b>2.96</b>	2.82	2.69	2.57	2.46	2.35	2.24	2.14	2.04	1.94	1.84
<b>-0.9</b>	2.82	<b>2.62</b>	2.43	2.29	2.16	2.05	1.91	1.8	1.69	1.58	1.48
<b>-0.8</b>	2.69	2.43	<b>2.2</b>	2.02	1.86	1.72	1.59	1.46	1.34	1.22	1.1
<b>-0.7</b>	2.57	2.29	2.02	<b>1.8</b>	1.61	1.45	1.3	1.15	1.02	0.89	0.77
<b>-0.6</b>	2.46	2.16	1.86	1.61	<b>1.4</b>	1.21	1.04	0.88	0.73	0.59	0.45
<b>-0.5</b>	2.35	2.05	1.72	1.45	1.21	<b>1</b>	0.81	0.63	0.47	0.31	0.17
<b>-0.4</b>	2.24	1.91	1.59	1.3	1.04	0.81	<b>0.6</b>	0.41	0.23	0.06	-0.1
<b>-0.3</b>	2.14	1.8	1.46	1.15	0.88	0.63	0.41	<b>0.2</b>	0	-0.18	-0.35
<b>-0.2</b>	2.04	1.69	1.34	1.02	0.73	0.47	0.23	0	<b>-0.2</b>	-0.39	-0.58
<b>-0.1</b>	1.94	1.58	1.22	0.89	0.59	0.31	0.06	-0.18	-0.39	<b>-0.6</b>	-0.79
<b>0</b>	1.84	1.48	1.1	0.77	0.45	0.17	-0.1	-0.35	-0.58	-0.79	<b>-1</b>
<b>0.1</b>	1.74	1.38	1	0.64	0.32	0.02	-0.25	-0.51	-0.75	<b>-0.98</b>	-0.79
<b>0.2</b>	1.65	1.28	0.89	0.53	0.19	-0.11	-0.4	-0.67	<b>-0.92</b>	-0.75	-0.58
<b>0.3</b>	1.56	1.18	0.78	0.41	0.07	-0.25	-0.54	<b>-0.82</b>	-0.67	-0.51	-0.35
<b>0.4</b>	1.47	1.08	0.68	0.3	-0.05	-0.37	<b>-0.68</b>	-0.54	-0.4	-0.25	-0.1
<b>0.5</b>	1.38	0.99	0.58	0.19	-0.17	<b>-0.5</b>	-0.37	-0.25	-0.11	0.02	0.17
<b>0.6</b>	1.29	0.89	0.48	0.09	<b>-0.28</b>	-0.17	-0.05	0.07	0.19	0.32	0.45



<b>0.7</b>	1.21	0.8	0.38	<b>-0.02</b>	0.09	0.19	0.3	0.41	0.53	0.64	0.77
<b>0.8</b>	1.12	0.71	<b>0.28</b>	0.38	0.48	0.58	0.68	0.78	0.89	1	1.1
<b>0.9</b>	1.04	<b>0.62</b>	0.71	0.8	0.89	0.99	1.08	1.18	1.28	1.38	1.48
<b>0.99</b>	<b>0.96</b>	1.04	1.12	1.21	1.29	1.38	1.47	1.56	1.65	1.75	1.84

**Table 1b.** Minimum values of  $\beta$  for given values of  $\delta$  and  $\gamma$ . b)  $0 < \gamma < 0.99$  and  $< -0.99$   
 $< \delta < 0.99$

$\gamma$	<b>0</b>	<b>0.1</b>	<b>0.2</b>	<b>0.3</b>	<b>0.4</b>	<b>0.5</b>	<b>0.6</b>	<b>0.7</b>	<b>0.8</b>	<b>0.9</b>	<b>0.99</b>
$\delta$											
<b>-0.99</b>	1.88	1.74	1.65	1.56	1.47	1.38	1.29	1.21	1.12	1.04	<b>0.96</b>
<b>-0.9</b>	1.48	1.38	1.28	1.18	1.08	0.99	0.89	0.8	0.71	<b>0.62</b>	1.04
<b>-0.8</b>	1.1	1	0.89	0.78	0.68	0.58	0.48	0.38	<b>0.28</b>	0.71	1.12
<b>-0.7</b>	0.77	0.64	0.53	0.41	0.3	0.19	0.09	<b>-0.02</b>	0.38	0.8	1.21
<b>-0.6</b>	0.45	0.32	0.19	0.07	-0.05	-0.17	<b>-0.28</b>	0.09	0.48	0.89	1.29
<b>-0.5</b>	0.17	0.02	-0.11	-0.3	-0.37	<b>-0.5</b>	-0.17	0.19	0.58	0.99	1.38
<b>-0.4</b>	-0.1	-0.25	-0.4	-0.5	<b>-0.68</b>	-0.37	-0.05	0.3	0.68	1.08	1.47
<b>-0.3</b>	-0.35	-0.51	-0.67	<b>-0.8</b>	-0.54	-0.25	0.07	0.41	0.78	1.18	1.56
<b>-0.2</b>	-0.58	-0.75	<b>-0.92</b>	-0.7	-0.4	-0.11	0.19	0.53	0.89	1.28	1.65
<b>-0.1</b>	-0.79	<b>-0.98</b>	-0.75	-0.5	-0.25	0.02	0.32	0.64	1	1.38	1.75

<b>0</b>	<b>-1</b>	-0.79	-0.58	-0.4	-0.1	0.16	0.45	0.77	1.1	1.48	1.84
<b>0.1</b>	-0.79	<b>-0.6</b>	-0.39	-0.2	0.06	0.31	0.59	0.89	1.22	1.58	1.94
<b>0.2</b>	-0.58	-0.39	<b>-0.2</b>	0	0.23	0.47	0.73	1.02	1.34	1.69	2.04
<b>0.3</b>	-0.35	-0.18	0	<b>0.2</b>	0.41	0.63	0.88	1.15	1.46	1.8	2.14
<b>0.4</b>	-0.1	0.06	0.23	0.41	<b>0.6</b>	0.81	1.04	1.3	1.59	1.91	2.24
<b>0.5</b>	0.17	0.31	0.47	0.63	0.81	<b>1</b>	1.21	1.45	1.72	2.05	2.35
<b>0.6</b>	0.45	0.59	0.73	0.88	1.04	1.21	<b>1.4</b>	1.61	1.86	2.16	2.46
<b>0.7</b>	0.77	0.89	1.02	1.15	1.3	1.45	1.61	<b>1.8</b>	2.02	2.29	2.57
<b>0.8</b>	1.1	1.22	1.34	1.46	1.59	1.72	1.86	2.02	<b>2.2</b>	2.43	2.68
<b>0.9</b>	1.48	1.58	1.69	1.8	1.91	2.05	2.16	2.29	2.43	<b>2.62</b>	2.82
<b>0.99</b>	1.84	1.94	2.04	2.14	2.24	2.35	2.46	2.57	2.68	2.82	<b>2.96</b>

## **Laminate Construction Considerations**

Parametric studies conducted by the authors have shown that the nondimensional parameters used in the present study are coupled functions of laminate stacking sequence and ply material properties. For example, a parametric plot is presented in Fig. 3, for the nine material systems given in Nemeth (2000), that shows the coupled dependence of  $\gamma$  and  $\delta$  on the fiber orientation angle  $\theta$  for  $[\pm\theta]_s$  laminates (see Fig. 1). Thus, practical restrictions on laminate construction can be used to determine relationships between the nondimensional parameters and "practical" bounds on their values.

In this section, upper-bound values for  $\alpha$ ,  $\beta$ ,  $\gamma$ , and  $\delta$  are determined. It was found that the bounding values for stiffness properties are obtained for laminates made of a single material because multiple materials reduce the overall stiffness properties, compared to those of the stiffest individual material. This result may be understood by appealing to a simple rule-of-mixtures approach. As such, hybrid materials are not considered in the present study and focus is placed solely on laminated composites in which each layer is made of the same material. In addition, bounds on the product of the anisotropy parameters and a practical envelope of their difference are presented that can be used to identify the extent of the design-parameter space.

To determine the desired bounds information, it is helpful to express the bending stiffnesses in terms of the material invariants,  $W_1$ - $W_5$ , and the lamination parameters,  $\xi_1$ - $\xi_{12}$ , (e.g. Miki, (1982) and Fukunaga and Hirano, (1982)) as follows

$$\begin{Bmatrix} D_{11} \\ D_{12} \\ D_{22} \\ D_{66} \\ D_{16} \\ D_{26} \end{Bmatrix} = \frac{t^3}{12} \begin{bmatrix} 1 & \xi_9 & \xi_{10} & 0 & 0 \\ 0 & 0 & -\xi_{10} & 1 & 0 \\ 1 & -\xi_9 & \xi_{10} & 0 & 0 \\ 0 & 0 & -\xi_{10} & 0 & 1 \\ 0 & \frac{\xi_{11}}{2} & \xi_{12} & 0 & 0 \\ 0 & \frac{\xi_{11}}{2} & -\xi_{12} & 0 & 0 \end{bmatrix} \begin{Bmatrix} W_1 \\ W_2 \\ W_3 \\ W_4 \\ W_5 \end{Bmatrix} \quad (21)$$

The lamination parameters are calculated from the following integrals

$$(\xi_9 \quad \xi_{10} \quad \xi_{11} \quad \xi_{12}) = \frac{3}{2} \int_{-1}^1 (\cos 2\theta \quad \cos 4\theta \quad \sin 2\theta \quad \sin 4\theta) u_i^2 du_i \quad (22)$$

where  $h_i$  is the distance of a particular ply surface from the mid plane,  $t$  is the thickness of the laminate,  $\theta$  is the ply angle (see Fig. 1) and  $u_i = 2h_i/t$ . The material invariants are linear functions of the ply stiffnesses,  $Q_{ij}$  (e.g. Jones, (1999)) and are given by

$$\begin{aligned} W_1 &= \frac{3Q_{11} + 3Q_{22} + 2Q_{12} + 4Q_{66}}{8} \\ W_2 &= \frac{Q_{11} - Q_{22}}{2} \\ W_3 &= \frac{Q_{11} + Q_{22} - 2Q_{12} - 4Q_{66}}{8} \\ W_4 &= \frac{Q_{11} + Q_{22} + 6Q_{12} - 4Q_{66}}{8} \\ W_5 &= \frac{W_1 - W_4}{2} \end{aligned} \quad (23)$$

The description of flexural stiffnesses in terms of ply stiffnesses and lamination parameters using Eqs. (21) and (22) is applicable to all linearly elastic anisotropic materials in a state of plane stress. As such, the applicability of the current work is broad and extends to plates made from many materials including: laminated continuously

reinforced composites; short fiber reinforced composites; functionally graded materials and homogeneous isotropic materials.

Next, it is useful to express  $\alpha$ ,  $\beta$ ,  $\gamma$ , and  $\delta$  in terms of material invariants and lamination parameters as follows

$$\alpha = \sqrt[4]{\frac{W_1 - \xi_9 W_2 + \xi_{10} W_3}{W_1 + \xi_9 W_2 + \xi_{10} W_3}} \quad (24)$$

$$\beta = \frac{W_1 - 3\xi_{10} W_3}{\left[ (W_1 + \xi_{10} W_3)^2 - \xi_9^2 W_2^2 \right]^{1/2}} \quad (25)$$

$$\gamma = \frac{\xi_{11}/2 W_2 + \xi_{12} W_3}{\sqrt[4]{(W_1 + \xi_9 W_2 + \xi_{10} W_3)^3 (W_1 - \xi_9 W_2 + \xi_{10} W_3)}} \quad (26)$$

$$\delta = \frac{\xi_{11}/2 W_2 - \xi_{12} W_3}{\sqrt[4]{(W_1 + \xi_9 W_2 + \xi_{10} W_3)(W_1 - \xi_9 W_2 + \xi_{10} W_3)^3}} \quad (27)$$

(i) *Upper Bounds on the Nondimensional Parameters*

Parametric studies indicate that the extreme values of  $\alpha$ ,  $\beta$ ,  $\gamma$ , and  $\delta$  are obtained for single-layer laminates, with ply angle  $\theta$ , or for cross-ply laminates ( $\theta = 0^\circ$  and  $90^\circ$ ). To determine the extreme values of the nondimensional parameters it is helpful to identify the ply angles that give extreme values of the lamination parameters,  $\xi_i$ . These

extreme values are given in Table 2. Clearly, the results in the table indicate that the extreme values of the nondimensional parameters are given solely in terms of the material invariants or the ply stiffnesses,  $Q_{ij}$ , by

$$\alpha_{\max} = \sqrt[4]{\frac{W_1 + W_2 + W_3}{W_1 - W_2 + W_3}} = \sqrt[4]{\frac{Q_{11}}{Q_{22}}} \quad (28)$$

where  $\xi_9 = -1$  and  $\xi_{10} = 1$ , which corresponds to  $\theta = 90^\circ$

$$\alpha_{\min} = \sqrt[4]{\frac{W_1 - W_2 + W_3}{W_1 + W_2 + W_3}} = \sqrt[4]{\frac{Q_{22}}{Q_{11}}} \quad (29)$$

where  $\xi_9 = 1$  and  $\xi_{10} = 1$ , which corresponds to  $\theta = 0^\circ$

$$\beta_{\max} = \frac{W_1 + 3W_3}{(W_1 - W_3)} = \frac{3(Q_{11} + Q_{22}) - 2Q_{12} - 4Q_{66}}{Q_{11} + Q_{22} + 2Q_{12} + 4Q_{66}} \quad (30)$$

where  $\xi_9 = 0$  and  $\xi_{10} = -1$ , which corresponds to  $\theta = \pm 45^\circ$

$$\beta_{\min} = \frac{W_1 - 3W_3}{(W_1 + W_3)} = \frac{2(Q_{12} + 2Q_{66})}{Q_{11} + Q_{22}} \quad (31)$$

where  $\xi_9 = 0$  and  $\xi_{10} = 1$ , which corresponds to  $(90_a, 0_b)_s$  or  $(0_a, 90_b)_s$ . The subscripts a and b indicate the fractional contribution of the plies to the total laminate thickness. Here, the subscript a =  $1 - 0.5^{1/3} \approx 0.206$  and the subscript b =  $0.5^{1/3} \approx 0.794$ .

**Table 2.** Lamination Parameters and their extreme values

Lamination Parameter	Ply Angle, $\theta$					
	0	45	60	90	-45	-60
$\xi_9(\cos 2\theta)$	1	0	0.5	-1	0	0.5
$\xi_{10}(\cos 4\theta)$	1	-1	-0.5	1	-1	-0.5
$\xi_{11}(\sin 2\theta)$	0	1	0.866	0	-1	-0.866
$\xi_{12}(\sin 4\theta)$	0	0	-0.866	0	0	0.866

The expressions given by Eqs. (28) - (31) show that the limiting values of the nondimensional parameters are determined by the basic ply stiffnesses,  $Q_{ij}$ . As such, materials with the greatest orthotropy ratios

$$\frac{Q_{11}}{Q_{22}} \quad (32a)$$

and

$$\frac{Q_{11}}{Q_{12} + 2Q_{66}} \quad (32b)$$

give the extreme values of the nondimensional parameters. Typically, for current materials, these ratios have values that range from 3 for a glass/epoxy material up to values near 80 for the graphite/epoxy P-100/AS3502 material (Nemeth, 2000). However, the upper-bound values of  $\alpha$  and  $\beta$  are defined if a material with infinite values of these ratios is considered. These considerations, and the previously obtained strain-energy considerations, yield

$$0 < \alpha < \infty \quad (33a)$$

and

$$-1 < \beta < 3 \quad (33b)$$

Equation (31) shows that  $\beta$  has a minimum value that approaches zero for composites constructed from conventionally reinforced unidirectional plies; that is, plies with  $Q_{12} > 0$ . This condition is in addition to the following thermodynamic requirements:  $Q_{11}$ ,  $Q_{22}$  and  $Q_{66} > 0$ , as given by Lempriere (1968). However, the second thermodynamic condition in Eq. (10) shows that  $\beta$  has a minimum value that approaches  $-1$ . It would be useful to identify the values of  $Q_{11}$ ,  $Q_{22}$ ,  $Q_{12}$  and  $Q_{66}$  that meet this requirement. To achieve such an extreme value requires that the (positive) stiffness  $Q_{66}$  vanishes so as to minimize the numerator in Eq. (31). The next step is to establish extreme values of  $Q_{12}$ . Lempriere (1968) gives the following thermodynamic requirement,

$$Q_{12}^2 < Q_{11}Q_{22} \quad (34)$$

that gives a minimum value of  $Q_{12} > -\sqrt{Q_{11}Q_{22}}$ . Substituting this condition into Eq. (31) yields

$$\beta_{\min} > -2 \frac{\sqrt{Q_{11}Q_{22}}}{Q_{11} + Q_{22}} \quad (35)$$

which is readily shown to give the minimum value,  $\beta_{\min} > -1$ , for  $Q_{11} = Q_{22}$ . As an aside, it is of interest to note that Eq. (35) shows that the minimum value of  $\beta$  is given by the negative ratio of geometric to arithmetic means of the principal stiffnesses. In



summary, to obtain the minimum value of  $\beta$ , a ply architecture is needed for which  $Q_{11} = Q_{22}$ ,  $Q_{12} \rightarrow -Q_{11}$  and  $Q_{66} \rightarrow 0$ , and for which  $Q_{16} = Q_{26} = 0$ . No ply architectures are currently known that meet these requirements.

The bounds on  $\beta$  given by Eq. (33b) are in contrast to those bounds given by Brunelle (1985) where bounds of  $0 < \beta < 1$  are suggested using a rules of mixture approach. Clearly, such bounds are overly limiting and if applied will significantly underestimate the potential for elastic tailoring.

Examination of Eqs. (26) and (27) indicates that the extreme values of the anisotropy parameters  $\delta$  and  $\gamma$  are given by an odd function of a single ply angle. This angle is a function of the material invariants but, because its complicated nature is not insightful, its expression is not presented herein. It is noted that the maximum value occurs in the vicinity of  $\theta = 50^\circ$  and  $40^\circ$ , for  $\delta$  and  $\gamma$ , respectively. The extreme values are found by substituting the maximum value for  $\beta$ ,  $\beta = 3$ , into Eq. (20) to yield

$$|\delta, \gamma| < 1 \quad (36)$$

This result may also be found from thermodynamic considerations by substituting  $\beta = 3$  and  $\nu_f = 1$  into the fourth and fifth expressions in Eq. (9).

Although Eq. (36) gives the individual bounds on  $\gamma$  and  $\delta$ , it does not provide information about their relative values. The curves in Fig. 3 suggest that additional information such as the bounds on their product and the maximum difference between their relative values would be very useful.

(ii) *Bounds on the Product of the Flexural Anisotropy Parameters*

Additional insight into the bounds on  $\delta$  and  $\gamma$  is obtained by considering bounds on the product, as represented by

$$\delta\gamma = \frac{D_{16}D_{26}}{D_{11}D_{22}} = \frac{\xi_{11}^2 / 4 W_2^2 - \xi_{12}^2 W_3^2}{(W_{12} + \xi_{10} W_3)^2 - \xi_9^2 W_2^2} \quad (37)$$

It is significant that the negative coefficient of  $\xi_{12}^2$  gives rise to the possibility of obtaining negative values of  $\delta\gamma$ , and as such, the lower-bound value is sought. To accomplish this task it is further noted that the lamination parameters may not be varied independently but must obey the following constraints (see Fukunaga and Sekine, 1992),

$$2\xi_9^2 - 1 \leq \xi_{10} \leq 1 - 2\xi_{11}^2 \quad (38)$$

and

$$2(1 + \xi_{10})\xi_{11}^2 - 4\xi_9\xi_{11}\xi_{12} + \xi_{12}^2 \leq [\xi_{10} - 2\xi_9^2 + 1](1 - \xi_{10}) \quad (39)$$

with each equality constraint obeying a trigonometric identity. Furthermore, the magnitudes of all lamination parameters are less than unity as deduced directly from their definition in Eq. (22).

An exhaustive trial-and-error search for combinations of  $\xi_9 - \xi_{12}$  that minimise  $\delta\gamma$  revealed that  $\xi_9 = \xi_{11} = 0$  and that  $\xi_{12}$  has a value close to unity. Furthermore, the

constraint on lamination parameters in Eq. (39) is satisfied by equating both sides of the inequality and reduces to

$$\xi_{12}^2 = 1 - \xi_{10}^2 \quad (40)$$

As such, the expression for  $\delta\gamma$  reduces to

$$\delta\gamma = \frac{D_{16}D_{26}}{D_{11}D_{22}} = -\frac{(1 - \xi_{10}^2)W_3^2}{(W_1 + \xi_{10}W_3)^2} \quad (41)$$

Differentiating Eq. (41) with respect to  $\xi_{10}$ , setting the resulting expression to zero, and rearranging, gives the optimal value of  $\xi_{10}$  as

$$\xi_{10}^{\text{opt}} = -\frac{W_3}{W_1} \quad (42)$$

Substituting Eq. (42) into Eq. (39) gives the minimal value for  $\delta\gamma$  as

$$(\delta\gamma)_{\min} = -\frac{W_3^2}{W_1^2 - W_3^2} \quad (43)$$

If a material under consideration has orthotropy ratios given by the expressions in Eq. (32) that approach infinity, a lower-bound value of  $\delta\gamma$  is obtained from Eq. (43) which is  $-0.125$ . Furthermore, Eqs. (42) and (40) give  $\xi_{10} = -0.33$  and  $\xi_{12} = 0.94$ , respectively. Finally,  $\xi_9 = 0$  and  $\xi_{11} = 0$ . A lay-up that closely matches these requirements is the 20-layer laminate represented by

$$[[(\theta, \theta + 90)_s]_2, \theta + 90, \theta + 90]_s$$

where  $\theta$  is close to  $22.5^\circ$ . An upper-bound value for  $\delta\gamma$  is obtained directly from Eq. (41) and shows that a value of unity may never be exceeded. Thus,  $\delta\gamma$  have limiting values given by

$$-0.125 \leq \delta\gamma < 1 \quad (44)$$

(iii) *Envelope of the Flexural Anisotropy Parameters*

Because of the coupled dependence of the flexural anisotropy parameters on the laminate construction characteristics, it is useful to know the maximum difference that can occur between the two parameters (see Fig. 3). This information is found by considering the maximum value of  $|\delta - \gamma|$  as a function of  $\delta$  (or  $\gamma$ ). Such calculations provide an envelope for the feasible region of  $\delta$  and  $\gamma$ . This task is achieved by maximizing  $|\delta - \gamma|$  for given values of  $\delta$  (or  $\gamma$ ).

To establish the location of the envelope of the feasible region requires a multi-step optimisation process. In the present study, a three-step optimisation process was used. The first step identifies values of the lamination parameters. The second step identifies the ply angles and the cubic volume fraction of each ply angle for the lamination parameters found in the first step. Finally, stacking sequences are found that provide the cubic volume fractions found in the second step.

First, it is noted that the parameters  $\delta$  and  $\gamma$  are functions of four variables; these are the lamination parameters,  $\xi_9$ - $\xi_{12}$ . Gradient-based optimisation methods were used to identify the values of  $\xi_9$ - $\xi_{12}$  that provide the maximum difference in the anisotropy parameters,  $|\delta - \gamma|_{\max}$ . Extensive numerical studies show that  $|\delta - \gamma|_{\max}$  is not given by a unique combination of the values of lamination-parameter values. One of the parameters can be chosen arbitrarily. In the present study, the value of  $\xi_9$  was set to zero for convenience. Furthermore, the numerical studies show that the condition given by Eq. (39) approaches an equality for  $|\delta - \gamma|_{\max}$ . As a result, the optimisation process simplifies to one containing two variables; that is, any two from  $\xi_9$ - $\xi_{12}$ . Once the combination of lamination parameters is found that gives  $\delta$  and  $\gamma$  values on the envelope of the feasible region, the corresponding stacking sequences must be identified. This task is done in the second step of the optimisation process.

Matching the stacking sequences to the optimal set of lamination parameters identified in step one is problematic because the lamination parameters are continuous functions and the lay-ups are composed of discrete plies. The implication is that it may not be possible to match exactly the optimal set of lamination parameters with that of a real lay-up. Trial and error shows that a match can be made sufficiently close such that the values of  $\delta$  and  $\gamma$  are within 1% of those calculated by using the optimal set of lamination parameters. To proceed, it is noted that the flexural lamination parameters, given in Eq. (22), are found as the summation of products of the cubic volume fraction,  $V_i$ , and an appropriate trigonometric term. It is the cubic volume fraction that has discrete values in a real lay-up. For example, if one unique ply angle is present, then the cubic volume fraction is unity and the summation contains only one term. If two ply angles are

present, then the summation contains two terms and the cubic volume fraction of both ply angles depends on the stacking sequence. Utilizing Eq. (22), the cubic volume fraction for a given ply angle is given by

$$V_i = \frac{3}{2} \int_{-1}^1 u_i^2 du_i \quad (45)$$

To establish lay-ups on the envelope of the feasible region, the number of unique ply angles is progressively increased until viable lay-ups are found. Starting with a single ply angle, it is observed from the expressions for  $\delta$  and  $\gamma$ , Eqs. (26) and (27), that it is impossible to obtain oppositely signed values of  $\delta$  and  $\gamma$ . As a consequence, the feasible region of  $\delta$  and  $\gamma$  containing a single ply angle is significantly reduced from that available. Using two unique ply angles allows the lamination parameters to be written as

$$\begin{aligned} \xi_9 &= V_1 \cos 2\theta_1 + V_2 \cos 2\theta_2 \\ \xi_{10} &= V_1 \cos 4\theta_1 + V_2 \cos 4\theta_2 \\ \xi_{11} &= V_1 \sin 2\theta_1 + V_2 \sin 2\theta_2 \\ \xi_{12} &= V_1 \sin 4\theta_1 + V_2 \sin 4\theta_2 \end{aligned} \quad (46a)$$

where

$$V_1 + V_2 = 1 \quad (46b)$$

When two unique ply angles are present, each lamination parameter becomes a function of three variables; that is  $\xi_i = \xi_i(\theta_1, \theta_2, V_1)$ . Essentially, the task is to find values of  $\theta_1$ ,  $\theta_2$ , and  $V_1$  that provide calculated lamination parameters that match the optimal set of lamination parameters found in the first step of the optimisation process. This task is done by using a gradient-based optimisation method. Importantly, it was found that two

unique ply angles were sufficient to match the optimal lamination parameters identified in the first step. The final step is to identify a stacking sequence that matches the optimal value of the cubic volume fraction,  $V_1$ . This step was done using the method outlined in Appendix 1. Interestingly, it was found that the minimum number of layers required in a symmetric laminate to obtain  $|\delta - \gamma|$  values that lie within 1% of  $|\delta - \gamma|_{\max}$  is twenty. This finding appears to be a new result; that is, any symmetric laminate composed of two unique ply angles must have a minimum of 20 layers to ensure stacking sequences provide material properties that lie within 1% of the theoretical optimum (as provided by lamination parameters).

Results that show the feasible region of the flexural anisotropy parameters for a material with an infinitely large orthotropy ratio  $Q_{11}/Q_{22}$  are presented in Fig. 4. The lower-bound curve in Fig. 4 was obtained by setting values of  $\delta$  from  $-1$  to  $1$ , in  $0.1$  increments, and conducting the first step of the optimisation process to maximize  $\delta - \gamma$ . In contrast, the upper-bound curve is found by setting values of  $\gamma$  from  $-1$  to  $1$ , in  $0.1$  increments, and maximizing  $\gamma - \delta$ . Interestingly, the largest difference in the anisotropy parameters,  $|\delta - \gamma|_{\max}$ , over the entire range of  $\delta$  and  $\gamma$  values is given by the same values that provide  $(\delta, \gamma)_{\min}$ , given by Eq. (43). For this case,  $\delta = -\gamma = 0.35$  and  $|\delta - \gamma|_{\max} = 0.7$ . Current composite materials have finite  $Q_{11}/Q_{22}$  ratios but nonetheless occupy a similar region to that shown in Fig. 4.

Further details of the results from each step of the optimisation process are shown in Table 3, where data is shown that was used to obtain the lower-bound curve in Fig. 4. Laminates, with stacking sequences comprising 20 layers, are listed that are located on the envelope of the feasible region. To obtain stacking sequences for the upper-bound curve in Fig. 4, it is necessary to add  $90^\circ$  to each ply angle in laminates listed in Table 3. It is then noted that the values of  $\delta$  and  $\gamma$  in Table 3 interchange.

**Table 3.** Laminate lay-ups on Lower Boundary of Feasible Region for  $\gamma$  and  $\delta$ , as shown in Fig. 4. Note that  $\xi_9 = 0$ .

$\xi_{10}$	$\xi_{11}$	$\xi_{12}$	$\gamma$	$\delta$	$\gamma\delta$	$\gamma-\delta$	$\theta_1$	$\theta_2$	$V_1$	Lay-up
-0.46	0.39	0.79	0.62	0.00	0.00	0.62	34.3	-68.5	0.67	[34.3 <sub>3</sub> , -68.5 <sub>5</sub> , 34.3 <sub>2</sub> ] <sub>s</sub>
-0.41	0.30	0.85	0.56	-0.10	-0.06	0.66	32.5	-67.2	0.62	[32.5 <sub>2</sub> , -67.2 <sub>2</sub> , 32.5 <sub>1</sub> , -
-0.36	0.19	0.91	0.49	-0.20	-0.10	0.69	30.6	-65.6	0.58	[30.6 <sub>2</sub> , -65.6 <sub>2</sub> , 30.6 <sub>1</sub> , -
-0.34	0.07	0.94	0.40	-0.30	-0.12	0.70	28.5	-63.8	0.53	[28.5 <sub>2</sub> , -63.8 <sub>4</sub> , 28.5 <sub>1</sub> , -
-0.34	-0.06	0.94	0.30	-0.40	-0.12	0.70	26.3	-61.6	0.47	[26.3 <sub>1</sub> , -61.6 <sub>2</sub> , 26.3 <sub>1</sub> , - 61.6 <sub>2</sub> , 26.3 <sub>1</sub> , -61.6 <sub>2</sub> , 26.3 <sub>1</sub> , -
-0.37	-0.21	0.90	0.18	-0.50	-0.09	0.68	24.1	-59.1	0.41	[24.1 <sub>1</sub> , -59.1 <sub>4</sub> , 24.1 <sub>1</sub> , -
-0.44	-0.36	0.81	0.03	-0.60	-0.02	0.63	21.9	-56.3	0.35	[21.9 <sub>1</sub> , -56.3 <sub>4</sub> , 21.9 <sub>1</sub> , -
-0.55	-0.52	0.67	-0.15	-0.70	0.11	0.55	19.9	-53.4	0.27	[19.9 <sub>1</sub> , -53.4 <sub>8</sub> , 19.9 <sub>1</sub> ] <sub>s</sub>
-0.69	-0.68	0.49	-0.38	-0.80	0.30	0.42	18.0	-50.5	0.19	[-50.5 <sub>4</sub> , 18.0 <sub>3</sub> , -



-0.84	-0.84	0.26	-0.66	-0.90	0.59	0.24	16.4	-47.7	0.10	[-47.7 <sub>5</sub> ,16.4 <sub>2</sub> ,-
-1	-1	0	-1	-1	1	0		-45	0	[-45 <sub>10</sub> ] <sub>s</sub>
-0.52	0.48	0.71	0.67	0.10	0.07	0.57	35.8	-69.7	0.71	[35.8 <sub>3</sub> ,-69.6 <sub>3</sub> ,35.8,-
-0.58	0.56	0.63	0.72	0.20	0.14	0.52	37.3	-70.6	0.74	[37.3 <sub>3</sub> ,-70.6 <sub>2</sub> ,37.3,-
-0.64	0.63	0.55	0.77	0.30	0.23	0.47	38.5	-71.6	0.78	[38.5 <sub>3</sub> ,-71.6 <sub>2</sub> ,38.5 <sub>4</sub> ,-
-0.70	0.69	0.47	0.81	0.40	0.32	0.41	39.7	-72.1	0.82	[39.7 <sub>4</sub> ,-72.1 <sub>3</sub> ,39.7 <sub>3</sub> ] <sub>s</sub>
-0.76	0.75	0.39	0.85	0.50	0.42	0.35	40.8	-72.8	0.85	[40.8 <sub>4</sub> ,-72.8 <sub>2</sub> ,40.8 <sub>4</sub> ] <sub>s</sub>
-0.81	0.81	0.31	0.88	0.60	0.53	0.28	41.8	-73.3	0.88	[41.8 <sub>4</sub> ,-73.3,41.8 <sub>2</sub> ,-73.3 <sub>3</sub> ] <sub>s</sub>
-0.86	0.86	0.23	0.91	0.70	0.64	0.21	42.7	-73.7	0.91	[42.7 <sub>5</sub> ,-73.7,42.7,-73.7 <sub>3</sub> ] <sub>s</sub>
-0.91	0.91	0.15	0.94	0.80	0.75	0.14	43.5	-74.2	0.94	[43.5 <sub>6</sub> ,-74.2 <sub>2</sub> ,43.5,-72.3] <sub>s</sub>
-0.96	0.96	0.07	0.97	0.90	0.88	0.07	44.3	-74.6	0.97	[44.3 <sub>7</sub> ,-74.6 <sub>3</sub> ] <sub>s</sub>
-1	1	0	1	1	1	0	45		1	[45 <sub>10</sub> ] <sub>s</sub>

### **Bounds on Buckling Resistance**

By enforcing thermodynamic requirements and considering practical laminate construction issues, bounds on the nondimensional flexural orthotropy and flexural anisotropy parameters have been found. For convenience, these bounds are listed as follows

$$0 < \alpha < \infty$$

$$-1 < \beta < 3$$

$$-1 < \nu_f < 1$$

$$-1 < \delta, \gamma < 1$$

$$-0.125 \leq \delta\gamma \leq 1$$

$$|\delta - \gamma|_{\max} = 0.7$$

By using these bounding values for the nondimensional parameters, upper bounds on the buckling resistance of plates can be found. To illustrate how these bounds are found, the buckling resistance of long, orthotropic plates with either simply supported edges or

clamped edges and subjected to compression, shear or pure bending is considered subsequently. The geometry and loading conditions for these cases are shown in Fig. 1.

(i) *Compression-Loaded Orthotropic Plate with Simply Supported Edges*

For this class of plates, the buckling resistance is expressed in terms of the nondimensional parameters and a nondimensional buckling coefficient  $K_x$  by

$$K_x = \frac{b^2 (N_x)^{cr}}{\pi^2 \sqrt{D_{11} D_{22}}} = 2(1 + \beta) \quad (47)$$

where  $(N_x)^{cr}$  is the buckling load per unit width and  $b$  is the plate width. This solution is exact and was first obtained by Huber (1929) in its dimensional form. Substituting  $-1 < \beta < 3$  into Eq. (47) indicates that

$$K_x < 8 \quad (48)$$

This result is valid for all potential materials, including those not yet discovered or developed, and clearly demonstrates the utility of knowing the bounds on the nondimensional parameters. In design, a more useful measure of buckling resistance is often needed because  $K_x$  is not an absolute buckling-resistance measure because of its dependence on the plate bending stiffnesses  $D_{11}$  and  $D_{22}$ . A more useful measure is given by the ratio of the buckling load for an arbitrary symmetrically laminated plate to that for the corresponding isotropic plate; that is,

$$\frac{(N_x)^{cr}}{(N_x)^{cr}_{iso}} = \frac{(D_{11}D_{22})^{1/2}}{D_{iso}} \frac{K_x}{K_{x(iso)}} \quad (49a)$$

or

$$\frac{(N_x)^{cr}}{(N_x)^{cr}_{iso}} = \varepsilon \frac{(1+\beta)}{2} \quad (49b)$$

where

$$\varepsilon = \frac{(D_{11}D_{22})^{1/2}}{D_{iso}} \quad (50)$$

and  $D_{iso}$  is the well-known bending stiffness of the corresponding isotropic plate. In Eqs. (49), the buckling load has been normalized with respect to the corresponding isotropic-plate value, which is indicated by the use of "iso" as a subscript. It is noted that every oriented material available in lamina form may be laminated into a material where the overall inplane elastic properties are effectively isotropic in nature. Such a normalization has the advantage of a direct comparison with the performance of the commonly used isotropic material. Furthermore, it is noted that  $\beta=1$  for an isotropic material and Eq. (47) gives  $K_{x(iso)} = 4$ . Noting that

$$D_{iso} = W_1 \frac{t^3}{12} \quad (51)$$

gives

$$\varepsilon = \frac{[(W_1 + \xi_{10}W_3)^2 - \xi_9^2 W_2^2]^{1/2}}{W_1} \quad (52)$$

Moreover,

$$\varepsilon_{\max} = \frac{W_1 + W_3}{W_1} = \frac{(Q_{11} + Q_{22})}{2W_1} \quad (53)$$

where  $\xi_9 = 0$  and  $\xi_{10} = 1$ , which corresponds to  $(90_{1-1/2}^{1/3}, 0_{1/2}^{1/3})_s$  or  $(0_{1-1/2}^{1/3}, 90_{1/2}^{1/3})_s$  lay-ups. Similarly,

$$\varepsilon_{\min} = \frac{[(W_1 + W_3)^2 - W_2^2]^{1/2}}{W_1} = \frac{(Q_{11}Q_{22})^{1/2}}{W_1} \quad (54)$$

which corresponds to  $(0^\circ)$  or  $(90^\circ)$  unidirectional lay-ups. However, the value of  $\varepsilon$  for a unidirectional lay-up with  $\theta = 45^\circ$  maximizes  $\beta$ , and as a result, maximizes the buckling loads. Specifically, the buckling loads for a unidirectional lay-up with  $\theta = 45^\circ$  are given by

$$\frac{(N_x)^{cr}}{(N_x)^{cr}_{iso}} = \frac{W_1 - W_3}{2W_1} \left[ 1 + \frac{W_1 + 3W_3}{(W_1 - W_3)} \right] \quad (55)$$

which is obtained by computing the material invariants and lamination parameters for  $\theta = 45^\circ$ , substituting the results into Eq. (52) for  $\varepsilon$  and Eq. (25) for  $\beta$ , and then

evaluating Eq. (50b) for the buckling-load ratio. For materials with infinite values of  $\frac{Q_{11}}{Q_{22}}$

and  $\frac{Q_{11}}{Q_{12} + 2Q_{66}}$ , which represents the bounds of feasibility, substituting Eqs. (32) into Eq.

(49) yields

$$\left( \frac{(N_x)^{cr}}{(N_x)^{cr}_{iso}} \right)_{\max} = \frac{4}{3} \quad (56)$$

which clearly shows that buckling resistance of an elastically tailored plate can never exceed 133% of that for the corresponding isotropic plate. However, it is important to note that the buckling resistance per unit mass is likely to be much larger for certain classes of materials.

(ii) *Compression-Loaded Orthotropic Plate with Clamped Edges*

There appears to be no closed form solution for this case. However, a least-squares-fit regression analysis made across the practical range of  $0 < \beta < 3$  with the analytical model described by Nemeth (2000) gives

$$K_x = 4.59 + 2.36\beta \quad (57)$$

as an expression for the buckling coefficient. This expression provides accuracy to within 1.3% of Nemeth's results. Fig. 5 shows the linear variation of  $K_x$  with  $\beta$  obtained by Nemeth (solid black line) and the close fit obtained by the regression formula (circular symbols), Eq. (57). Using similar analysis to that previously considered for simply supported edges gives

$$K_x < 11.67 \quad (58)$$

as the bound on the possible buckling coefficients and

$$\frac{(N_x)^{cr}}{(N_x)^{cr}_{iso}} = \frac{W_1 - W_3}{6.95W_1} \left[ 4.59 + 2.36 \frac{W_1 + 3W_3}{(W_1 - W_3)} \right] \quad (59)$$

for the nondimensionalised buckling load, noting that buckling loads are maximised (as they were for simply supported edges) for  $\theta = 45^\circ$ . For materials with infinite values of

$\frac{Q_{11}}{Q_{22}}$  and  $\frac{Q_{11}}{Q_{12} + 2Q_{66}}$ , substituting Eqs. (32) into Eq. (57) yields

$$\left( \frac{(N_x)^{cr}}{(N_x)^{cr}_{iso}} \right)_{\max} = 1.12 \quad (60)$$

which clearly shows that buckling resistance of an elastically tailored plate can never exceed 112% of that for the corresponding isotropic plate for clamped edges. In comparison with case of simply supported edges, there is significantly reduced ability for elastically tailoring. However, it is noted that is extremely difficult to obtain fully clamped edge restraint in practice.

(iii) *Shear-Loaded Orthotropic Plate with Simply Supported Edges*

An approximate closed-form solution for this loading case may be obtained by making a quadratic least-square regression analysis, using the practical range of  $0 < \beta < 3$  in the analytical model presented by Nemeth (1997). This process gives

$$K_{xy} = \frac{(N_{xy})^{cr} b^2}{\pi^2 (D_{11} D_{22}^3)^{1/4}} = 3.32 + 2.16\beta - 0.16\beta^2 \quad (61)$$

as an expression for the shear buckling coefficient. This formula gives results that are within 1% of Nemeth's results and a comparison is shown in Fig. 6. In this figure, the solid gray curve is the one obtained by Nemeth and the square symbols correspond to Eq. (61). The quadratic dependency of  $K_{xy}$  on  $\beta$  is also evident from Fig. 6. Using analysis similar to that used for the prior cases for compression loading gives

$$K_{xy} < 8.36 \quad (62)$$

for the upper bound on the possible range of buckling coefficients. Like for the compression-loaded plates,  $K_{xy}$ , is not an absolute buckling-resistance measure because of its dependence on  $D_{11}$  and  $D_{22}$ . A more useful measure is found by comparing the buckling load for an arbitrary symmetrically laminated plate with that for the corresponding isotropic plate; that is,

$$\frac{(N_{xy})^{cr}}{(N_{xy})^{cr}_{iso}} = \frac{(D_{11}D_{22}^3)^{1/4}}{D_{iso}} \frac{K_{xy}}{K_{xy(iso)}} \quad (63)$$

or

$$\frac{(N_{xy})^{cr}}{(N_{xy})^{cr}_{iso}} = \phi \frac{(3.32 + 2.16\beta - 0.16\beta^2)}{5.32} \quad (64a)$$

where

$$\phi = \frac{(D_{11}D_{22}^3)^{1/4}}{D_{iso}} \quad (64b)$$



Furthermore,  $K_{xy(\text{iso})} = 5.32$  for the isotropic case which compares with the value of 5.33 first obtained by Skan and Southwell (1924). Noting that,

$$\phi = \frac{\left[ (W_1 - \xi_9 W_2 + \xi_{10} W_3)^3 (W_1 + \xi_9 W_2 + \xi_{10} W_3) \right]^{1/4}}{W_1} \quad (65)$$

gives

$$\phi_{\max} = \frac{\left[ \left( W_1 + \frac{W_2}{2} + W_3 \right)^3 \left( W_1 - \frac{W_2}{2} + W_3 \right) \right]^{1/4}}{W_1} = \frac{\left[ (3Q_{11} - Q_{22})^3 Q_{11} \right]^{1/4}}{2\sqrt{2}W_1} \quad (66a)$$

corresponding to  $[90_{1-1/4}^{1/3}, 0_{1/4}^{1/3}]_s$  and

$$\phi_{\min} = \frac{\left[ (W_1 - W_2 + W_3)^3 (W_1 + W_2 + W_3) \right]^{1/4}}{W_1} = \frac{(Q_{11} Q_{22}^3)^{1/4}}{W_1} \text{ with } \xi_9 = 1 \text{ and } \xi_{10} = 1 \quad (66b)$$

corresponding to a single layer of  $0^\circ$ .

The expression for buckling load, Eq. (63), is readily simplified to one in two variables,  $\xi_9$  and  $\xi_{10}$ , by directly substituting for  $\beta$  from Eq. (25). Furthermore, the maximum buckling-load ratio is given on the bounds of feasible design space between  $\xi_9$  and  $\xi_{10}$ , which is given by the equality condition given by the constraint in Eq. (38). It is readily shown that for materials with infinitely large values of the orthotropy ratios,  $\frac{Q_{11}}{Q_{22}}$

and  $\frac{Q_{11}}{Q_{12} + 2Q_{66}}$ , yields a single ply orientation,  $\theta=60^\circ$ , with  $\xi_9 = \xi_{10} = -0.5$ , as the optimal lay-up. Furthermore, this lay-up lies within 1% of the optimal for all common material systems for which  $\frac{Q_{11}}{Q_{22}}$  and  $\frac{Q_{11}}{Q_{12} + 2Q_{66}} > 3.5$ . As such, the maximum buckling load is found by substituting this fiber orientation into Eq. (63) to obtain

$$\frac{(N_{xy})^{cr}}{(N_{xy})^{cr}_{iso}} = \frac{(W_1 + 0.5W_2 - 0.5W_3)^{1/2} \left[ (W_1 - 0.5W_3)^2 - 0.25W_2^2 \right]^{1/4}}{5.32W_1} \times \left( 3.32 + 2.16 \frac{W_1 + 3/2 W_3}{\left[ (W_1 - 0.5W_3)^2 - 0.25W_2^2 \right]^{1/2}} - 0.16 \frac{(W_1 + 3/2 W_3)^2}{\left[ (W_1 - 0.5W_3)^2 - 0.25W_2^2 \right]} \right) \quad (67)$$

For materials with infinitely large orthotropy ratios,  $\frac{Q_{11}}{Q_{22}}$  and  $\frac{Q_{11}}{Q_{12} + 2Q_{66}}$ , then

$$\left( \frac{(N_{xy})^{cr}}{(N_{xy})^{cr}_{iso}} \right)_{\max} = 1.36 \quad (68)$$

which clearly shows that buckling resistance of an elastically tailored plate with simply supported edges under shear loading can never exceed 136% of that for the corresponding isotropic plate. This finding is similar to that for the compression-loaded plates with simply supported edges.

(iv) *Shear-Loaded Orthotropic Plate of Infinite Length with Clamped Edges*

An approximate-closed form solution for this loading case was also obtained by making a quadratic least-squares fit for the practical range of  $0 < \beta < 3$ , to the results presented by Nemeth (1997). This fit gives

$$K_{xy} = \frac{(N_{xy})^{cr} b^2}{\pi^2 (D_{11} D_{22}^3)^{1/4}} = 6.13 + 3.02\beta - 0.19\beta^2 \quad (69)$$

as an expression for the shear buckling coefficient. This formula gives results that are within 0.5% of Nemeth's results and a comparison is shown in Fig. 6. In this figure, the solid black curve is the one obtained by Nemeth and the circular symbols correspond to Eq. (69). The quadratic dependency of  $K_{xy}$  on  $\beta$  is also evident from Fig. 6. Again, using analysis similar to that used for the prior cases gives

$$K_{xy} < 13.48 \quad (70)$$

for the upper bound on the possible range of buckling coefficients. Similar arguments to that presented for the plates with simply supported edges, reveals that  $\theta = 60^\circ$  is, once again, the corresponding optimal lay-up. As such,

$$\frac{(N_{xy})^{cr}}{(N_{xy})^{cr_{iso}}} = \frac{(W_1 + 0.5W_2 - 0.5W_3)^{1/2} \left[ (W_1 - 0.5W_3)^2 - 0.25W_2^2 \right]^{1/4}}{8.96W_1} \times \left( 6.13 + 3.02 \frac{W_1 + \frac{3}{2}W_3}{\left[ (W_1 - 0.5W_3)^2 - 0.25W_2^2 \right]^{1/2}} - 0.19 \frac{\left( W_1 + \frac{3}{2}W_3 \right)^2}{\left[ (W_1 - 0.5W_3)^2 - 0.25W_2^2 \right]} \right) \quad (71)$$

For materials with infinitely large values for the orthotropy ratios  $\frac{Q_{11}}{Q_{22}}$  and  $\frac{Q_{11}}{Q_{12} + 2Q_{66}}$ ,

$$\left( \frac{(N_{xy})^{cr}}{(N_{xy})^{cr}_{iso}} \right)_{\max} = 1.30 \quad (72)$$

Thus, the buckling resistance of an elastically tailored plate with clamped edges under shear loading can never exceed 130% of that for the corresponding isotropic plate.

(v) *Pure Inplane Bending of an Orthotropic Plate with Simply Supported Edges*

An approximate closed-form solution for this loading case was also obtained by making a quadratic least-square fit, for  $0 < \beta < 3$ , to the results presented by Nemeth (1997). This fit gives

$$K_b = \frac{b^2 (N_b)^{cr}}{\pi^2 \sqrt{D_{11} D_{22}}} = 13.42 + 10.85 \beta \quad (73)$$

as an expression for the buckling coefficient, where  $(N_b)^{cr}$  is the critical magnitude of the applied stress resultant at the edge. This simple formula provides accuracy to within 0.3% of Nemeth's results, which are given by the solid gray line in Fig. 7. The linear variation of  $K_b$  with  $\beta$  and the close fit obtained by the regression formula (square symbols) is also shown in Fig. 7.

Using analysis similar to that used for the previous cases gives

$$K_b < 45.97 \quad (74)$$

for the upper bound on the range of possible buckling coefficients and

$$\frac{(N_b)^{cr}}{(N_b)^{cr}_{iso}} = \frac{W_1 - W_3}{24.27W_1} \left[ 13.42 + 10.85 \frac{W_1 + 3W_3}{(W_1 - W_3)} \right] \quad (75)$$

for the nondimensionalized buckling load, noting that buckling loads are maximized (as they were for uniaxial compression) for  $\theta = 45^\circ$ . For materials with infinite values of

$\frac{Q_{11}}{Q_{22}}$  and  $\frac{Q_{11}}{Q_{12} + 2Q_{66}}$ , substituting Eqs. (32) into Eq. (76) yields

$$\left( \frac{(N_b)^{cr}}{(N_b)^{cr}_{iso}} \right)_{\max} = 1.26 \quad (76)$$

Similar to the other case, this result clearly shows that buckling resistance of an elastically tailored plate with simply supported edges under pure inplane bending can never exceed 126% of that for the corresponding isotropic plate.

(vi) *Pure Inplane Bending of an Orthotropic Plate with Clamped Edges*

A quadratic least-squares fit, for  $0 < \beta < 3$ , to the results presented by Nemeth (1997) gives

$$K_b = 26.85 + 12.61\beta \quad (77)$$

for the buckling coefficient and provides accuracy to within 1.7%. The linear variation of  $K_b$  with  $\beta$  and the close fit obtained by the regression formula for this case is also shown in Fig. 7. In particular, the solid black curve is Nemeth's results and the circular symbols correspond to Eq. (77). Likewise, it was found that

$$K_b < 64.68 \quad (78)$$

is the upper bound on buckling coefficients and

$$\frac{(N_b)^{cr}}{(N_b)^{cr}_{iso}} = \frac{W_1 - W_3}{39.46W_1} \left[ 26.85 + 12.61 \frac{W_1 + 3W_3}{(W_1 - W_3)} \right] \quad (79)$$

for the normalized buckling load, again noting that buckling loads are maximized (as they were for uniaxial compression) for  $\theta = 45^\circ$ . Once again, for materials with infinite values

of  $\frac{Q_{11}}{Q_{22}}$  and  $\frac{Q_{11}}{Q_{12} + 2Q_{66}}$ , substituting Eqs. (32) into Eq. (79) yields

$$\left( \frac{(N_b)^{cr}}{(N_b)^{cr}_{iso}} \right)_{\max} = 1.09 \quad (80)$$

Thus, the buckling resistance of an elastically tailored plate with clamped edges and subjected to pure inplane bending can never exceed 109% of that for the corresponding isotropic plate.

### **Concluding Remarks**

Nondimensional parameters and equations governing the buckling behavior of rectangular symmetrically laminated plates have been presented. These nondimensional parameters can be used to represent the buckling resistance of rectangular plates, made of all known linearly elastic structural materials, in a very general, insightful, and encompassing manner. In addition, these parameters can be used to assess the degree of

plate orthotropy, to assess the importance of anisotropy that couples bending and twisting deformations, and to characterize quasi-isotropic laminates quantitatively. Bounds for these nondimensional parameters have also been presented that are based on thermodynamics and practical laminate construction considerations. Additionally, the envelope of the practical design-parameter space for bending-twisting anisotropy has been presented. Knowing these bounds provides insight into potential gains in buckling resistance through laminate tailoring and composite-material development. As an illustration of this point, some of the bounds presented herein have been used to determine upper bounds on the buckling resistance of long rectangular orthotropic plates with simply supported or clamped edges and subjected to uniform axial compression, uniform shear, or pure inplane bending loads. The results indicate that the maximum gain in buckling resistance for orthotropic plates, with respect to the corresponding isotropic plate, through laminate tailoring is in the range of 26-36% for plates with simply supported edges, irrespective of the loading conditions considered. For plates with clamped edges, the corresponding gains in buckling resistance are in the range of 9-12% elastic tailoring for plates subjected to compression or pure inplane bending loads. For clamped plates subjected to shear loads, there is potentially a 30% increase in buckling resistance to be gained through laminate tailoring.

## **References**

Brunelle, E. J. and Oyibo, G. A., 1983. Generic Buckling Curves for Specially Orthotropic Rectangular Plates, *AIAA Journal*. **21**(8), 1150-1156.

Brunelle, E. J., 1985. The Fundamental Constants of Orthotropic Affine Slab/Plate Equations, *AIAA Journal*. **23**(12), 1957-1961.

Brunelle, E. J., 1986. Eigenvalue Similarity Rules for Symmetric Cross-Ply Laminated Plates, *AIAA Journal*. **24**(1), 151-154.

Chamis, C. C., 1969. Buckling of Anisotropic Composite Plates. *Journal of the Structural Division*, ASCE, **95**, 2119-2139.

Fukunaga, H. and Hirano, Y., 1982. Stability Optimization of Laminated Composite Plates under In-Plane Loads, *Proceedings of the Fourth International Conference on Composite Materials*, Vol. 1, 565-572

Fukunaga, H. and Sekine, H., 1992. Stiffness Design Method of Symmetric Laminates Using Lamination Parameters, *AIAA Journal*, Vol. 30, No. 11, 2791-2793.

Geier, B. and Singh, G., 1997. Some Simple Solutions for Buckling Loads of Thin and Moderately Thick Cylindrical Shells and Panels Made of Laminated Composite Material, *Aerospace Science and Technology*, **1**, 47-63.

Grenestedt, J. L., 1991. Lay-up Optimisation against Buckling of Shear Panels, *Structural Optimisation*, Vol **3**(7), 115-120.



- Huber , M. T., 1929, *Problem der Statik Technisch Wichtiger Orthotroper Platten*,  
Warsaw.
- Jones, R. M. 1999, *Mechanics of Composite Materials*, 2<sup>nd</sup> Edition, Philadelphia, Taylor  
and Francis
- Lempriere, B.M., 1968. Poisson's Ratio in Orthotropic Materials", *AIAA Journal*, **6**(11),  
2226-2227.
- Mansfield, E.H. 1989. *The Bending and Stretching of Plates*, 2<sup>nd</sup> Edition, Cambridge  
University Press Cambridge, UK.
- Miki, M., 1982. Material Design of Composite Laminates with Required in-Plane Elastic  
Properties, *Proceedings of the Fourth International Conference on Composite Materials*,  
Vol. 2, pp. 1725-1731.
- Nemeth, M. P., 1986. Importance of Anisotropy on Buckling of Composite-  
Loaded Symmetric Composites Plates. *AIAA Journal* **24**(11), 1831.
- Nemeth, M. P., 1992a. Buckling Behaviour of Long Symmetrically Laminated Plates  
subject to Combined Loadings, *NASA TP-3195*.

Nemeth, M. P., 1992b. Nondimensional Parameters and Equations for Buckling of Symmetrically Laminated Thin Elastic Shallow Shells, *NASA TM-104060*.

Nemeth, M. P., 1994. Nondimensional Parameters and Equations for Buckling of Anisotropic Shallow Shells. *ASME J. of Applied Mechanics* **61**(9), 664-669.

Nemeth, M. P., 1995. Buckling Behavior of Long Anisotropic Plates subject to Combined Loads, *NASA TP-3568*.

Nemeth, M. P., 1997. Buckling Behavior of Long Symmetrically Laminated Plates subjected to Shear or Linearly Varying Axial Loads, *NASA TP-3659*.

Nemeth, M. P., 2000. Buckling Behaviour of Long Symmetrically Laminated Plates subjected to Restrained Thermal Expansion and Mechanical Loads, *J. Thermal Stresses*, **23**, 873-916.

Oyibo, G. A. and Berman, J., 1985. Influence of Warpage on Composite Aeroelastic Theories, *AIAA/ASME/ASCE/AHS 26th Structures, Structural Dynamics and Materials Conference*, Orlando, FL, April 15-17, 1985. AIAA Paper No. 85-0673-CP

Skane, S. W. and Southwell, R. V., 1924. On the Stability under Shearing Stresses of a Flat Elastic Strip, *Proc. Roy. Soc. London, series A*, **105**, 582-607.

Shulesko, P., 1957. A Reduction Method for Buckling Problems of Orthotropic Plates, *The Aeronautical Quarterly*, **8**, May, 145-156.

Stein, M., 1983. Postbuckling of Orthotropic Composite Plates Loaded in Compression, *AIAA Journal*, **12** (12), 1729-1735.

Tsai, S. W. and Pagano, N. J., 1968. Invariant Properties of Composite Materials, *Composite Materials Workshop*, US Air Force, University of California at Berkeley, pp. 233-253.

Weaver, P. M., 2003. On Optimisation of Long Anisotropic Flat Plates subject to Compression Buckling Loads, *Proc. American Society of Composites 18<sup>th</sup> Technical conference*, paper 142, University of Florida.

Weaver, P. M., 2004. On Optimisation of Long Anisotropic Flat Plates subject to Shear Buckling Loads, *Proc. 45<sup>th</sup> AIAA, ASCE, ASME, AHS Structures Structural Dynamics and Materials conference*, Palm Springs, April, USA.

Wittrick, W.H., 1952. Correlation Between some Stability Problems for Orthotropic and Isotropic Plates under Bi-axial and Uni-axial Direct Stress, *The Aeronautical Quarterly*, **4**, August, 83-92.

Yang, I.-H. and Kuo, W.-S., 1986. The Global Constants in Orthotropic Affine Space, J. of the Chinese Society of Mechanical Engineers, 7(5), 355-360.

Zwillinger D., 1996. Standard Mathematical Tables and Formulae, CRC Press, 30<sup>th</sup> Edition, Boca Raton, Florida, USA.

## Appendix 1. Method for Determining Stacking Sequences

The cubic volume fractions of each ply within a 20-ply symmetric laminate are shown in Fig. A1, noting that only the top half of the laminate is shown because of symmetry.

	Layer 10	$1^3 - 0.9^3 = 0.271$
	Layer 9	$0.9^3 - 0.8^3 = 0.217$
	Layer 8	$0.8^3 - 0.7^3 = 0.169$
	Layer 7	$0.7^3 - 0.6^3 = 0.127$
	Layer 6	$0.6^3 - 0.5^3 = 0.091$
	Layer 5	$0.5^3 - 0.4^3 = 0.061$
	Layer 4	$0.4^3 - 0.3^3 = 0.037$
	Layer 3	$0.3^3 - 0.2^3 = 0.019$
	Layer 2	$0.2^3 - 0.1^3 = 0.007$
midplane	Layer 1	$0.1^3 - 0^3 = 0.001$

Figure A1. Cubic Volume fractions of each ply within a 20-layer symmetric laminate

To illustrate the method for obtaining lay-ups the stacking sequence for the laminate in the first row of Table 2 is sought. It is observed from the table that the cubic volume fraction of one of the unique ply angles is given by  $V_1 = 0.67$ . The strategy is to find those plies whose cubic volume fractions sum to 0.67 (or as close to this value as we can obtain). This summation is achieved by sequentially searching all permutations of ply positions. Trial and error shows it is most advantageous to start the process by including those plies with the largest cubic volume fractions. In this way, the outer 3 layers of the laminate (layers 8-10) have total cubic volume fraction of  $0.271 + 0.217 + 0.169 = 0.657$ . Subtracting this subtotal from our target value of 0.67 leaves a remaining cubic volume fraction of 0.013. By closely scrutinising the cubic volume fractions in Fig. A1, it is evident that the remaining cubic volume fraction of 0.13 cannot be matched exactly. In fact, the closest value that may be obtained is by including layers 1 and 2 with subtotal of 0.008. By adding both subtotals gives a total cubic volume fraction of 0.665. Although, this total does not match the required value, it is sufficiently accurate for our purposes because the difference in  $\delta$  and  $\gamma$  values (that depend on the cubic volume fraction), is less than 1 per cent. As such, the stacking sequence obtained is sufficiently accurate and is listed in the final column of the first row of Table 2. The remaining stacking sequences in Table 2 are calculated from cubic volume fractions in a similar way.

List of Figures

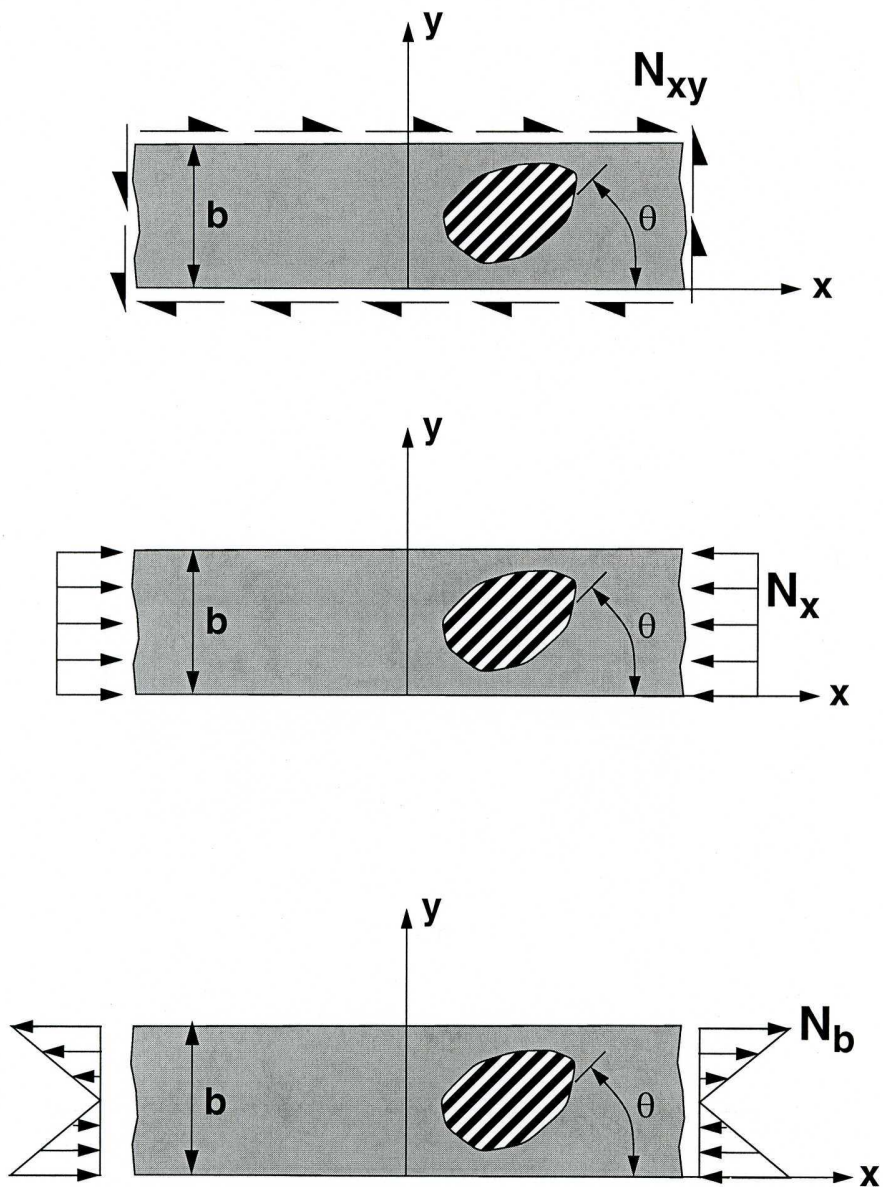


Figure 1. Load cases and geometry of rectangular plates

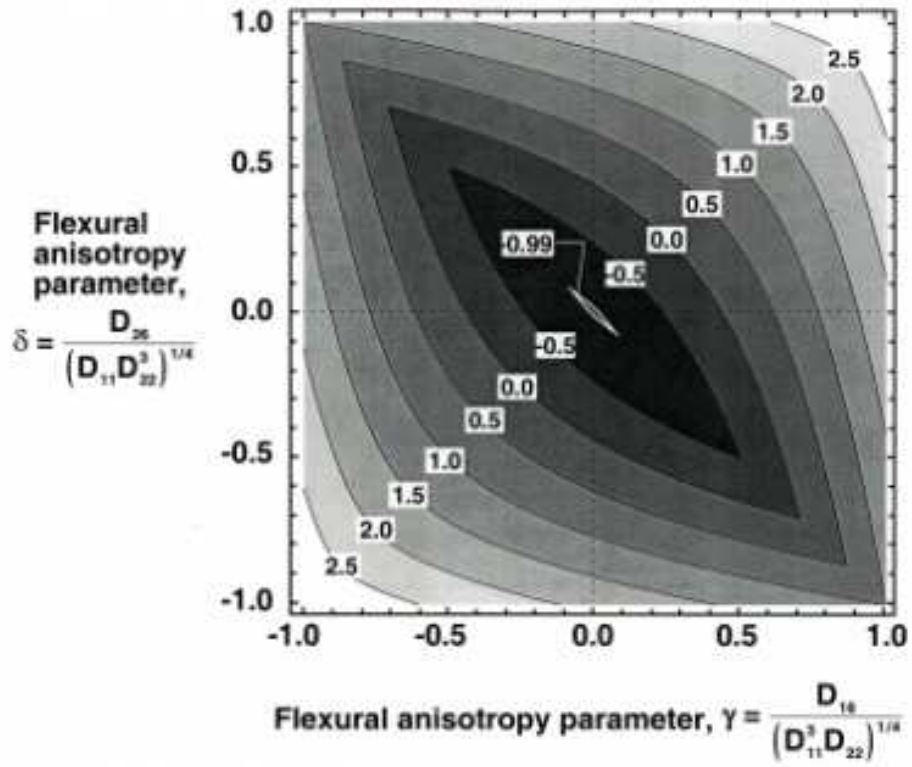


Figure 2. Contours of minimal values of  $\beta$  as a function of  $\delta$  and  $\gamma$ .



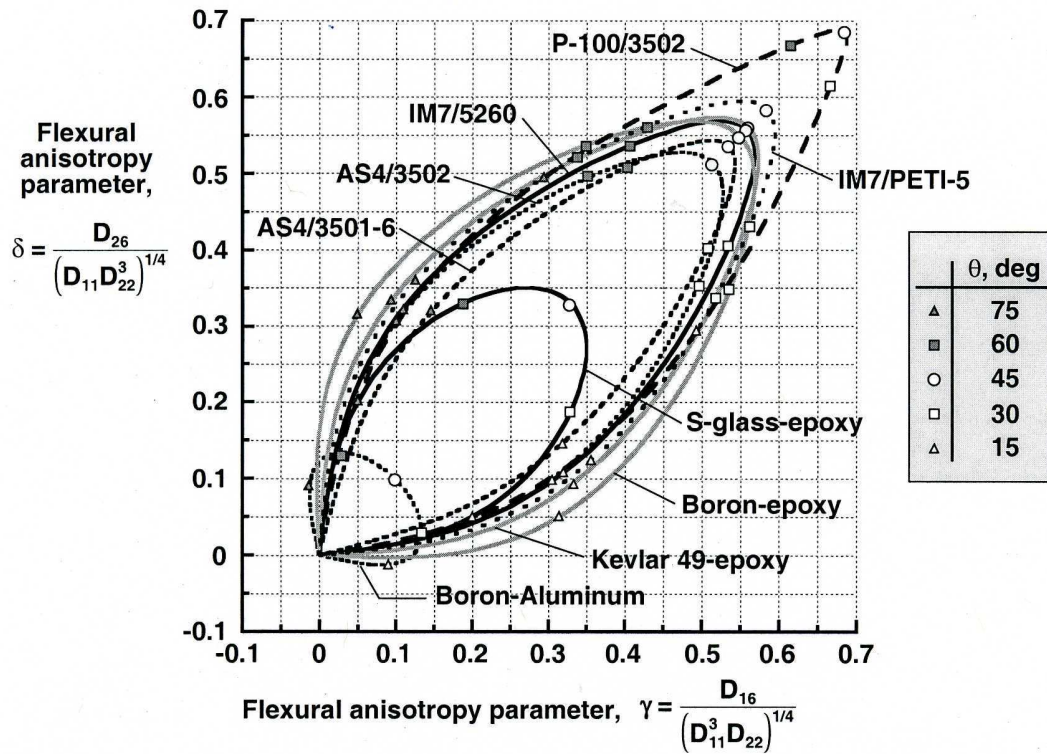


Figure 3. The coupled dependence of  $\gamma$  and  $\delta$  on the fiber orientation angle  $\theta$  for  $[+\theta]_s$  laminates, for different laminated composite materials

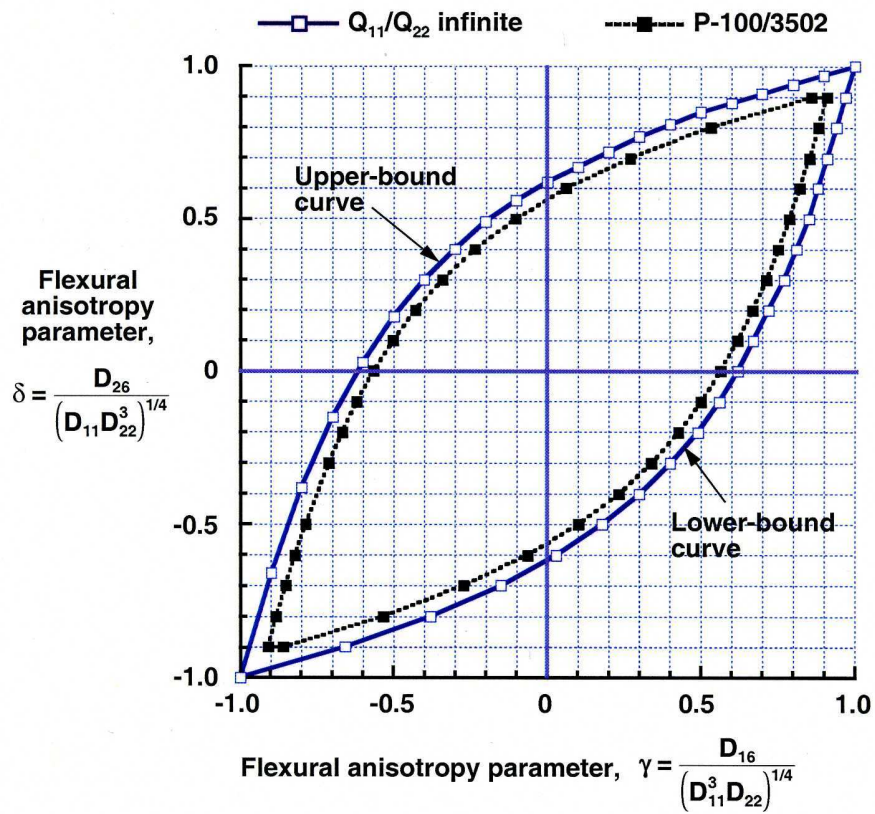


Figure 4. Feasible region of  $\delta$  and  $\gamma$ .

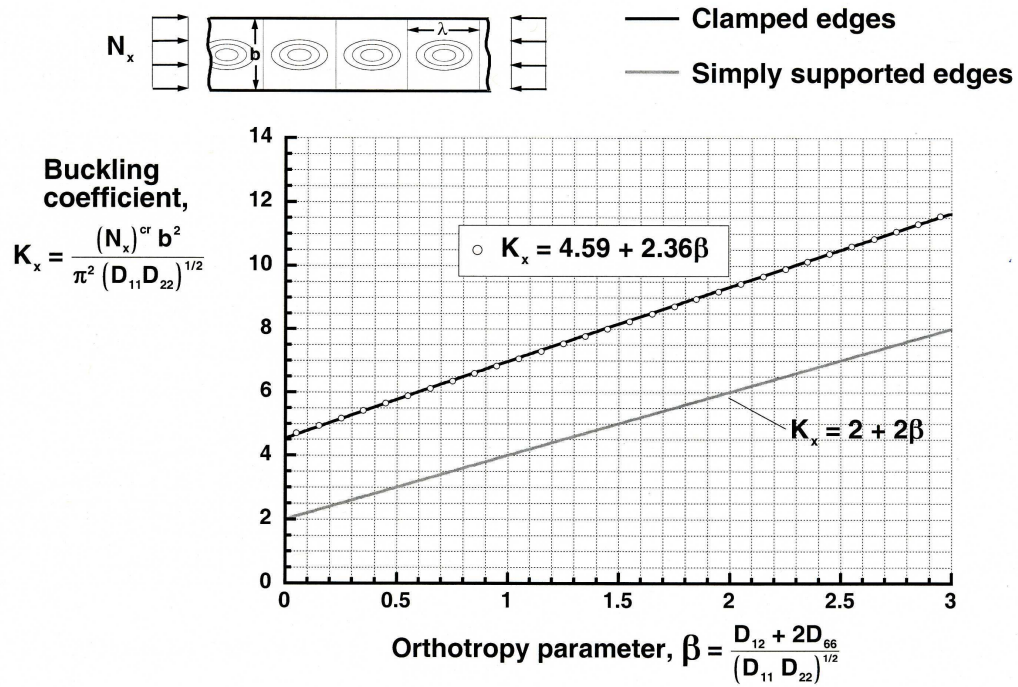


Figure 5. Variation of buckling coefficient,  $K_x$  with flexural-orthotropy parameter,  $\beta$ .

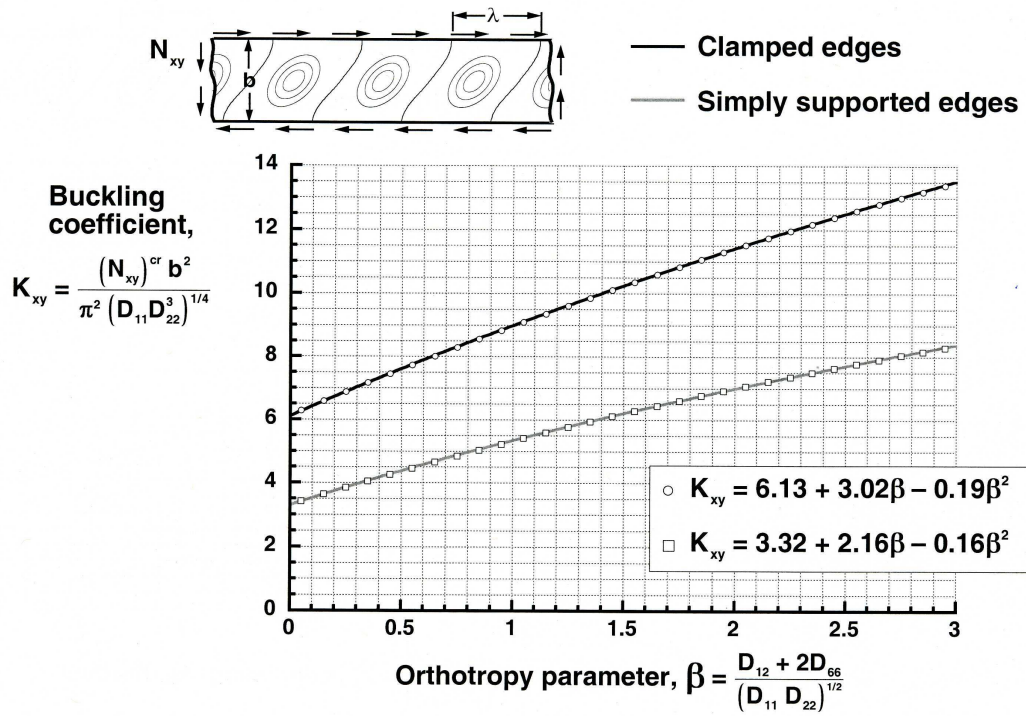


Figure 6. Variation of buckling coefficient,  $K_{xy}$  with flexural-orthotropy parameter,  $\beta$ .

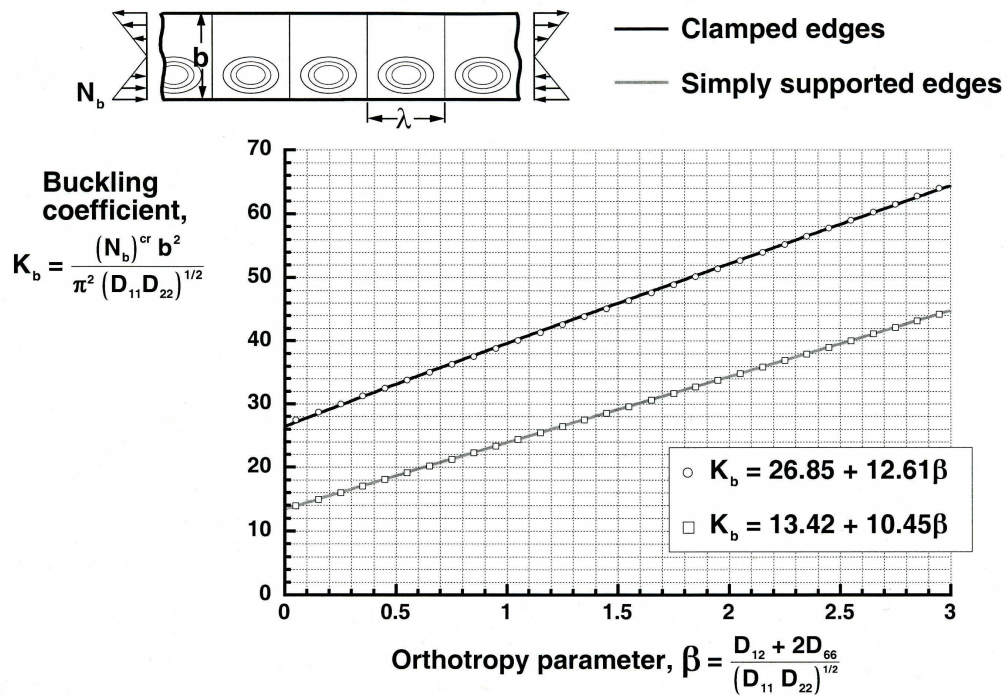


Figure 7. Variation of buckling coefficient,  $K_b$  with flexural-orthotropy parameter,  $\beta$ .